Expression and Gene Amplification of Actinin-4 in Invasive Ductal Carcinoma of the Pancreas

Satoru Kikuchi,[1,3] Kazufumi Honda,[1] Hitoshi Tsuda,[6] Nobuyoshi Hiraoka,[2] Issei Imoto,[4] Tomoo Kosuge,[5] Tomoko Umaki,[1] Kaoru Onozato,[6] Miki Shitashige,[1] Umio Yamaguchi,[1] Masaya Ono,[1] Akihiko Tsuchida,[3] Tatsuya Aoki,[3] Johji Inazawa,[4] Setsuo Hirohashi,[1,2] and Tesshi Yamada[1]

Abstract **Purpose:** An invasive growth pattern is one of the hallmarks of pancreatic ductal carcinoma. Actinin-4 is an actin-binding protein associated with enhanced cell motility, invasive growth, and lymph node metastasis. Actinin-4 might play an important role in the development and progression of pancreatic cancer.

Experimental Design: The expression of actinin-4 was examined immunohistochemically in 173 cases of invasive pancreatic ductal carcinoma. The copy number of the actinin-4 (*ACTN4*) gene was calculated by fluorescence *in situ* hybridization. The expression of actinin-4 was stably knocked down by short hairpin RNA, and tumorigenicity was evaluated by orthotopic implantation into mice with severe combined immunodeficiency.

Results: The expression level of actinin-4 was increased in 109 (63.0%) of 173 cases of pancreatic cancer. Kaplan-Meier survival curves revealed that patients with increased expression of actinin-4 had a significantly poorer outcome ($P = 0.00001$, log-rank test). Multivariate analysis by the Cox proportional hazard model showed that high expression of actinin-4 was the most significant independent negative predictor of survival (hazard ratio, 2.33; $P = 0.000009$). Amplification (defined as more than four copies per interphase nucleus) of the *ACTN4* gene was detected in 11 (37.9%) of 29 cases showing increased expression of actinin-4. Knockdown of actinin-4 expression inhibited the destructive growth of cancer cells in the pancreatic parenchyma.

Conclusion: Recurrent amplification of chromosome 19q13.1-2 has been reported in pancreatic cancer, but the exact target gene has not been identified. Actinin-4 contributes to the invasive growth of pancreatic ductal carcinoma, and *ACTN4* is one of the candidate oncogenes in this chromosome locus.

Invasive ductal carcinoma of the pancreas is one of the most aggressive forms of human malignancy, with a 5-year survival rate of <5% to 10% and a median survival of <6 months (1, 2). As a result, pancreatic cancer is the fourth leading cause of cancer death in the United States, and is the fifth in Japan (3). Massive local invasion to adjacent organs and/or metastasis to regional lymph nodes and distal organs are detected in the majority of patients at the time of diagnosis. To improve the prognosis of patients with pancreatic cancer, it will be necessary to elucidate the molecular mechanisms causing invasion and metastasis.

We have identified an actin-binding protein, actinin-4, as a biomarker of cancer invasion and metastasis (4). The expression of actinin-4 was closely associated with the invasive phenotype of breast cancer and was a prognostic indicator in patients with this disease (4). A microarray analysis revealed that actinin-4 was a significant prognostic indicator in patients with non–small cell lung cancer (5). The expression level of actinin-4 protein was increased in the majority of cases of colorectal cancer, and the increase in expression was most significant in dedifferentiated cancer cells infiltrating at the invasive front (6). In mouse models, colorectal cancer cells expressing actinin-4 showed infiltrative growth and metastasized into regional lymph nodes (6).

Oncogenic activation of the K-ras (*KRAS*) gene occurs in >90% of pancreatic ductal carcinomas and is detected even in premalignant intraepithelial lesions (7, 8). Transgenic mice with a K-ras^{G12D} transgene develop hyperplasia of ductal epithelial cells (9), but the hyperplastic lesions infrequently

Authors' Affiliations: [1]Chemotherapy Division, Cancer Proteomics Project and [2]Pathology Division, National Cancer Center Research Institute, [3]Third Department of Surgery, Tokyo Medical University, [4]Department of Molecular Cytogenetics, Tokyo Medical and Dental University, [5]Hepatobiliary and Pancreatic Surgery Division, National Cancer Center Central Hospital, Tokyo, Japan, and [6]Department of Pathology, National Defense Medical College, Tokorozawa, Japan

Received 1/9/08; revised 3/26/08; accepted 4/21/08.

Grant support: "Program for Promotion of Fundamental Studies in Health Sciences" conducted by the National Institute of Biomedical Innovation of Japan, grants from the Ministry of Health, Labor, and Welfare of Japan and the Ministry of Education, Culture, Sports, Science, and Technology of Japan, and generous grants from the Naito Foundation, the Princess Takamatsu Cancer Research Fund, and the Foundation for the Promotion of Cancer Research.

The costs of publication of this article were defrayed in part by the payment of page charges. This article must therefore be hereby marked *advertisement* in accordance with 18 U.S.C. Section 1734 solely to indicate this fact.

Note: Supplementary data for this article are available at Clinical Cancer Research Online (http://clincancerres.aacrjournals.org/).

Requests for reprints: Tesshi Yamada, Chemotherapy Division and Cancer Proteomics Project, National Cancer Center Research Institute, 5-1-1 Tsukiji, Chuo-ku, Tokyo 104-0045, Japan. Phone: 81-33542-2511; Fax: 81-33547-6045; E-mail: tyamada@gan2.res.ncc.go.jp.

doi:10.1158/1078-0432.CCR-08-0075

Table 1. Prognostic significance of actinin-4 expression in 173 cases of invasive ductal carcinoma of the pancreas

	Univariate analysis*			Multivariate analysis*		
	Hazard ratio	95% Confidence interval	P †	Hazard ratio	95% Confidence interval	P †
Age (y)						
<65/≥65	1.18	0.85-1.65	0.321584			
Gender						
Male/female	1.12	0.80-1.57	0.515322			
UICC stage ‡						
I-II/III-IV	2.59	1.31-5.12	0.006191	1.35	0.59-3.08	0.471917
Extent of primary tumor ‡						
T_{1-2}/T_{3-4}	1.81	1.16-2.82	0.008528	0.86	0.52-1.44	0.572695
Lymph node metastasis ‡						
N_0/N_1	2.73	1.82-4.08	0.000001	1.96	1.20-3.19	0.007271
Distant metastasis ‡						
M_0/M_1	2.40	1.68-3.44	0.000002	1.73	1.18-2.54	0.005023
Lymphatic invasion§						
ly0/ly1-3	2.06	1.44-2.95	0.000076	1.54	1.03-2.28	0.033537
Intrapancreatic nerve invasion§						
ne0/ne1-3	1.26	0.89-1.77	0.189521			
Macroscopic type§						
Nodular/infiltrative	1.28	0.91-1.80	0.162522			
Cancer-stroma relationship§						
Medullary and intermediate/scirrhous	1.14	0.81-1.60	0.458187			
Expression of actinin-4						
Positive/negative	2.27	1.57-3.27	0.000012	2.33	1.61-3.39	0.000009

*Univariate and multivariate analyses with Cox proportional hazards model.
† $P < 0.01$ was considered statistically significant.
‡ Based on the International Union Against Cancer tumor-node-metastasis classification (6th edition).
§ Based on the Japan Pancreas Society's classification of pancreatic carcinoma (2nd English edition).

progress into invasive tumors, suggesting that additional genetic events must occur for the development of fully malignant pancreatic tumors (10). Recurrent amplification of the chromosome locus 19q13.1-2 has been reported in pancreatic cancer cell lines and primary pancreatic cancers (11-13). Earlier studies indicated that the *AKT2* gene was the target of amplification, but *AKT2* was not always overexpressed in pancreatic cancer cell lines with gene amplification (14, 15), and its down-regulation by small interfering RNA did not significantly affect cell viability (16), leaving the precise target gene(s) of the 19q13.1-2 amplicon undetermined.

The histopathology of pancreatic cancer invariably reveals massive infiltration of small cancer nests lacking a glandular structure. This invasive growth pattern seems to be an intrinsic feature of pancreatic carcinogenesis and might reflect a specific underlying genetic alteration. The *ACTN4* gene that encodes actinin-4 has been mapped to chromosome 19q13[7] in the vicinity of the amplification described above (13). On the basis of these histopathologic and genetic observations, we hypothesized that the *ACTN4* gene might be a target of the 19q13.1-2 amplification and may play a significant role in the invasive growth of pancreatic ductal carcinoma. Because gene amplification is known to activate several oncogenes by increasing their expression levels (17), we first investigated the expression of actinin-4 in clinical samples of pancreatic cancer in order to assess the clinical relevance of any expression changes.

Patients and Methods

Immunohistochemistry. Immunohistochemical analysis was done on tissue specimens from 173 patients with pancreatic ductal carcinoma who had undergone surgical resection between 1990 and 2003 at the National Cancer Center Hospital (Tokyo, Japan) without any prior therapy. The tumors were staged according to the International Union Against Cancer (UICC) tumor-node-metastasis classification (18). Other pathologic variables (macroscopic type, lymphatic invasion, intrapancreatic nerve invasion, and cancer-stroma relationship; Table 1) were categorized according to the Japan Pancreas Society's classification of pancreatic carcinoma (19). The mean follow-up period was 25.7 months (ranging from 1 to 171 months). The protocol of this study was reviewed and approved by the institutional ethics committee.

Formalin-fixed paraffin-embedded tissue sections (5 μm thick) were stained by the immunoperoxidase method with avidin-biotin complex as described previously (20). We confirmed the absence of nonspecific staining by omitting the first antibody. Immunohistochemical results were judged by three investigators (S. Kikuchi, K. Honda, and N. Hiraoka) who were unaware of the clinical data.

Cell lines. All pancreatic cancer cell lines used in this study (BxPC3, AsPc-1, Mpanc96, Panc-1, MIA-PACA2, CFPAC-1, Capan-1, Capan-2, HPAC, Su86.86, and MIA-PACA) were obtained from the American Type Culture Collection.

Antibodies. Anti-actinin-4 rabbit polyclonal (Ab-2) and anti-E-cadherin mouse monoclonal (HECD-1) antibodies were generated as described previously (6, 21). Anti-pan AKT rabbit polyclonal

[7] http://www.ncbi.nlm.nih.gov/mapview/

antibody was purchased from Cell Signaling Technology. Anti-AKT2 mouse monoclonal antibody (F-7) was purchased from Santa Cruz Biotechnology. Anti-β-actin mouse monoclonal antibody (AC-15) was purchased from Abcam. Anti-Ki67 antigen mouse monoclonal antibody (MiB-1) was purchased from Dako.

Western blot analysis. Cells were extracted with lysis buffer [10 mmol/L HEPES (pH 7.4), 150 mmol/L NaCl, 1 mmol/L EDTA, 1% Triton X-100, 1% NP40, and 1 mg/mL NaN_3] containing a protease inhibitor cocktail (Sigma-Aldrich) on ice for 30 min. Cell lysates were separated by SDS-PAGE and transferred to Immobilon-P membranes (Millipore). After incubation with primary antibodies at 4°C overnight and relevant secondary antibodies at room temperature for 1 h, the reaction was detected with enhanced chemiluminescence Western blotting detection reagents (Amersham Biosciences; ref. 22). Blot

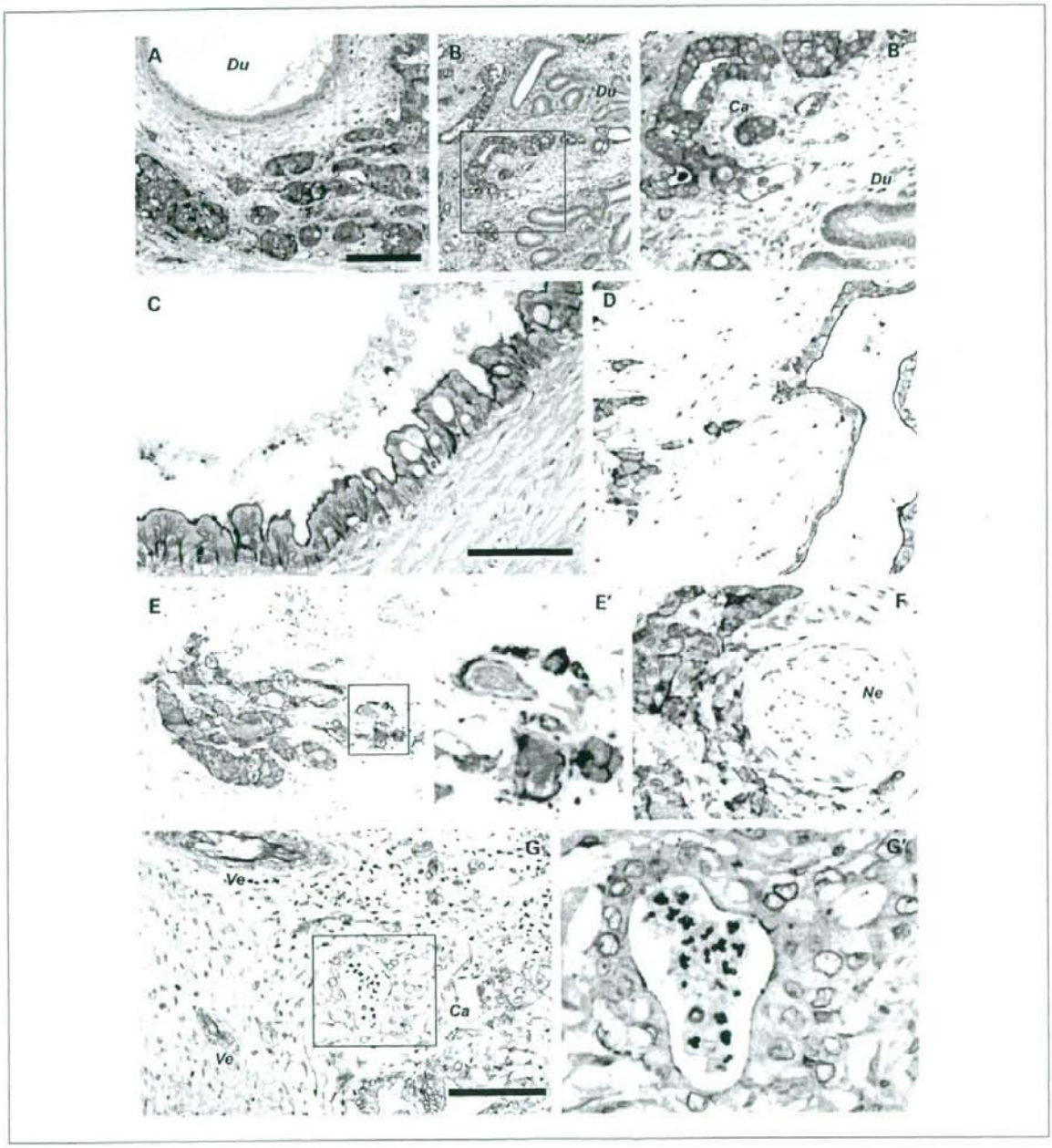

Fig. 1. Expression of actinin-4 in pancreatic cancer. Immunoperoxidase staining of actinin-4 in clinical samples of pancreatic cancer. *B'*, *E'*, and *G'*, insets from *B*, *E*, and *G*, respectively. Du, nonneoplastic pancreatic duct; Ca, cancer; Ne, peripheral nerve; Ve, blood vessels. Bars, 100 μm (*A* and *G*). Bar, 50 μm (*C*).

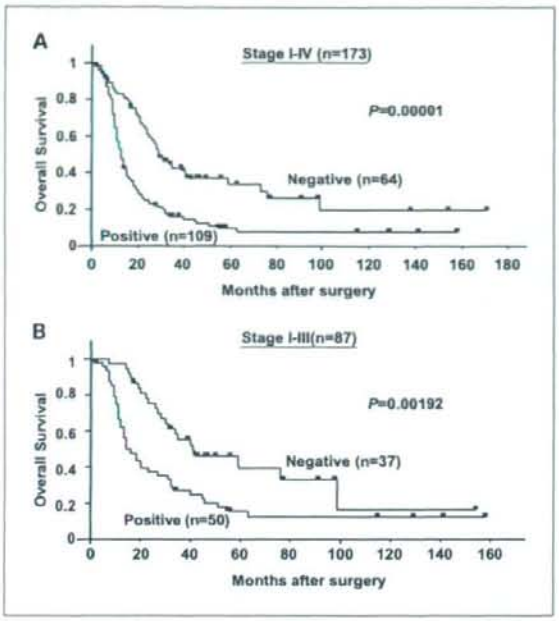

Fig. 2. Survival curves of patients positive and negative for actinin-4 expression. *A*, Kaplan-Meier analysis of overall survival for patients with clinical stage I to IV pancreatic ductal carcinoma (n = 173). Actinin-4 expression – positive cases (n = 109) had significantly poorer prognosis than expression-negative cases (n = 64; P = 0.00001, log-rank test). *B*, Kaplan-Meier analysis of overall survival for patients with clinical stage I to III pancreatic ductal carcinoma (n = 87). Actinin-4 expression – positive cases (n = 50) had significantly poorer prognosis than expression-negative cases (n = 37; P = 0.00192, log-rank test).

intensity was quantified with a LAS-3000 image analyzer and Multi-Gauze software (Fuji Film; ref. 23).

Fluorescence in situ hybridization analysis. Fluorescence *in situ* hybridization was done using the methods for PathVysion DNA probe kit (Abbott Molecular) as described previously (24). A representative formalin-fixed paraffin-embedded tissue block was selected by a pathologist (N. Hiraoka) and cut into 5-μm-thick sections. Hybridization was done at 37°C for 14 to 18 h with the denatured *ACTN4* (RP11-118P21) or *AKT2* (CTB-166E20) locus-containing bacterial artificial chromosome probe labeled with SpectrimOrange (Abbott Molecular). The specimen was counterstained with 4,6-dianidino-2-phenylindone. The number of fluorescence signals in 20 interphase tumor cell nuclei were counted independently by at least two investigators (S. Kikuchi and H. Tsuda or K. Onozato) and averaged.

Establishment of actinin-4 knockdown clones. *ACTN4* knockdown clones were established by the stable transfection of short hairpin RNA into BxPC-3 cells. A synthesized double-stranded oligonucleotide (5′-ggatggtcttgccttcaat-3′) targeting *ACTN4* mRNA was cloned into the pBAsi-hU6 Neo plasmid (Takara Bio), and the cells were transfected with LipofectAMINE 2000 reagent (Invitrogen). Twenty-four hours later, the transfection medium was replaced with RPMI 1640 containing 0.4 mg/mL of G418 (Geneticin, Invitrogen) to select clones with neomycin resistance.

Fluorescence cytochemistry. Cells grown on collagen-coated cover glasses (Asahi Technoglass) were fixed with 4% paraformaldehyde for 30 min at room temperature. The cells were incubated with anti–E-cadherin mouse monoclonal antibody and then with anti-mouse IgG Alexa Fluor 488 (Invitrogen). Filamentous actin fibers were visualized with Alexa Fluor 488 phalloidin (Invitrogen; ref. 25).

Scanning electron microscopy, cell migration assay, and cell growth assay. These assays and procedures are available online in the "Supplementary Methods."

Animal experiments. Female severe combined immunodeficiency mice (C.B-17/IcrCrl-scid) were purchased from Clea Japan and maintained in a specific pathogen-free environment. A laparotomy was done under general anesthesia, and 1×10^6 cells were injected orthotopically into the parenchyma of the pancreas with fine tuberculin needles, as described previously (26). The mice were sacrificed 5 weeks later, and serial sections of the entire pancreas were stained using H&E. The maximum diameter of the tumors was measured under a dissecting microscope (Nikon Instruments). All animal experimental procedures were reviewed and approved by the ethics committee of the National Cancer Center Research Institute (Tokyo, Japan).

Statistical analyses. Statistical analyses, including Kaplan-Meier analysis with log-rank test, χ^2 test, and the Cox proportional hazards regression model, were done with the StatFlex statistics package (version 5.0; Artiteck). The Wilcoxon rank sum test was done using a tool in the *R* project software package.[8]

Results

Expression of actinin-4 in invasive ductal carcinoma of the pancreas. The expression of actinin-4 protein was examined immunohistochemically in surgical specimens from 173 patients with pancreatic cancer (Fig. 1). The actinin-4 expression level in pancreatic cancer cells was increased compared with nonneoplastic duct epithelial cells (Fig. 1A and B). The expression of actinin-4 was limited to the apical and lateral membranes of cancer cells showing intraepithelial spreading (Fig. 1C), but this polarized distribution seemed to be lost in cancer cells that were dissociated from the glandular structure (Fig. 1D). Intense actinin-4 staining was observed in the periphery of cancer nests and in the membrane of solitary cells infiltrating the stroma (Fig. 1E and F).

Western blot analysis detected the expression of actinin-4 protein in 9 out of 11 (81.8%) pancreatic cancer cell lines examined, whereas AKT2 protein was detected only in Panc-1 cells (Supplementary Fig. S1).

Clinical significance of actinin-4 expression in pancreatic cancer. The staining intensity of actinin-4 was classified as "positive" when the actinin-4 expression level was equal to or higher than that of vascular endothelial cells, and "negative" when it was less than that of vascular endothelial cells (Fig. 1G). Of the 173 cases, there were 109 (63.0%) actinin-4 expression-positive cases and 64 (37.0%) expression-negative cases. The overall survival of positive cases was significantly worse than that of negative cases (P = 0.00001, log-rank test; Fig. 2A). Even in the 87 patients with clinical stages I to III, actinin-4 expression-positive cases had significantly poorer outcome than did expression-negative cases (P = 0.00192; Fig. 2B). Thirty-one (28.4%) out of the 109 actinin-4 expression-positive cases and 24 (37.5%) of the 64 actinin-4 expression-negative cases received postoperative chemotherapy (gemcitabine and others). There was no statistically significant difference in this respect between the groups (P = 0.2167, χ^2 test).

Univariate analysis with the Cox proportional hazards model (Table 1) revealed that clinical stage (P = 0.0062), extent of

[8] http://www.r-project.org

primary tumor (P = 0.0085), lymph node metastasis (P = 0.000001), distant metastasis (P = 0.000002), lymphatic invasion (P = 0.000076), and immunoreactivity of actinin-4 (P = 0.000012) were significantly correlated with the prognosis of the 173 patients with pancreatic cancer. Multivariate analysis indicated that actinin-4 expression was the most significant independent predictor of unfavorable prognosis (P = 0.000009; hazard ratio, 2.33; 95% confidence interval, 1.61-3.39),

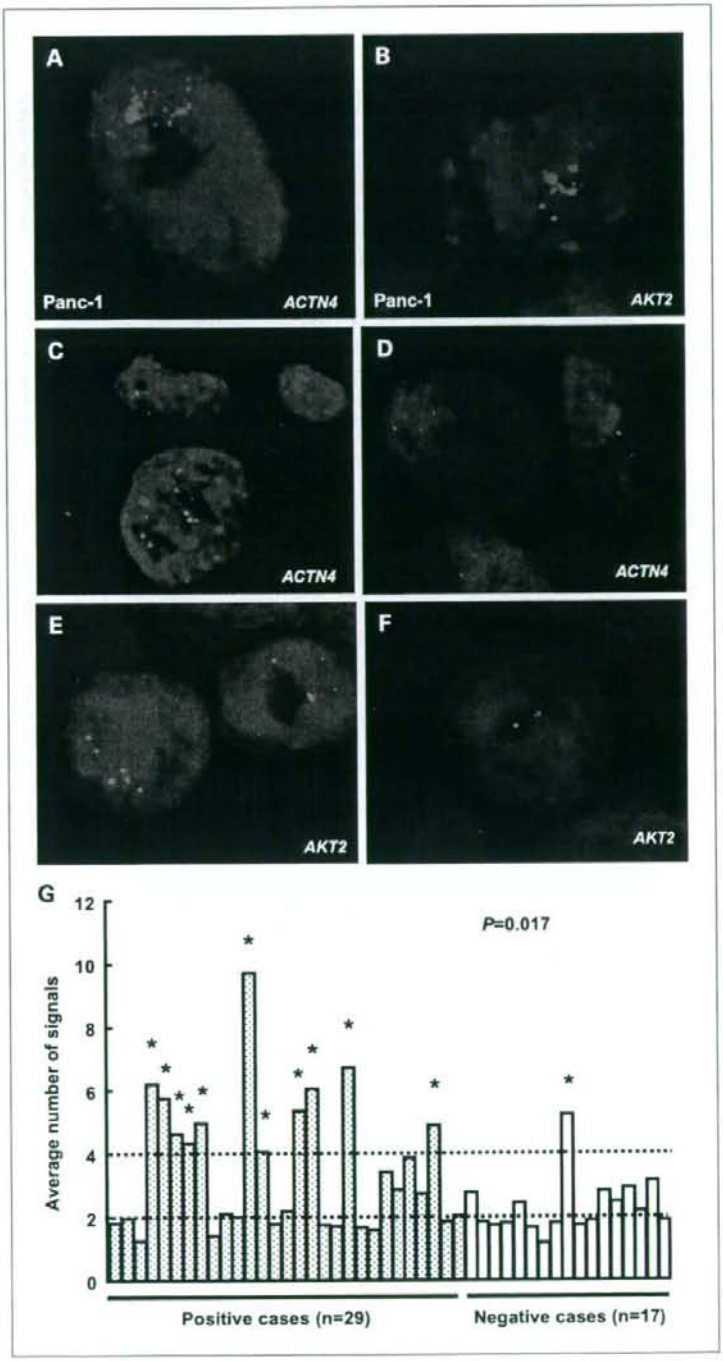

Fig. 3. Amplification of the *ACTN4* and *AKT2* genes in pancreatic cancer. *A-F*, fluorescence *in situ* hybridization analysis of copy numbers of the *ACTN4* (*A*, *C*, and *D*) and *AKT2* (*B*, *E*, and *F*) genes in a pancreatic cancer cell line (*Panc-1*; *A* and *B*) and clinical samples of pancreatic cancer (*C-F*). Increased copy numbers of the *ACTN4* (*C*) and *AKT2* (*E*) genes; two copies of the *ACTN4* (*D*) and *AKT2* (*F*) genes. *G*, correlation of actinin-4 protein expression and gene amplification. Average copy number of the *ACTN4* gene determined by fluorescence *in situ* hybridization in actinin-4 expression – positive cases (*gray columns*, n = 29) and expression-negative cases (*unshaded columns*, n = 17). Average signal number of <4 (per interphase nucleus) was defined as gene amplification (*). There is a significantly higher frequency of *ACTN4* amplification in actinin-4 expression – positive cases than in expression-negative cases (P = 0.017, χ^2 test).

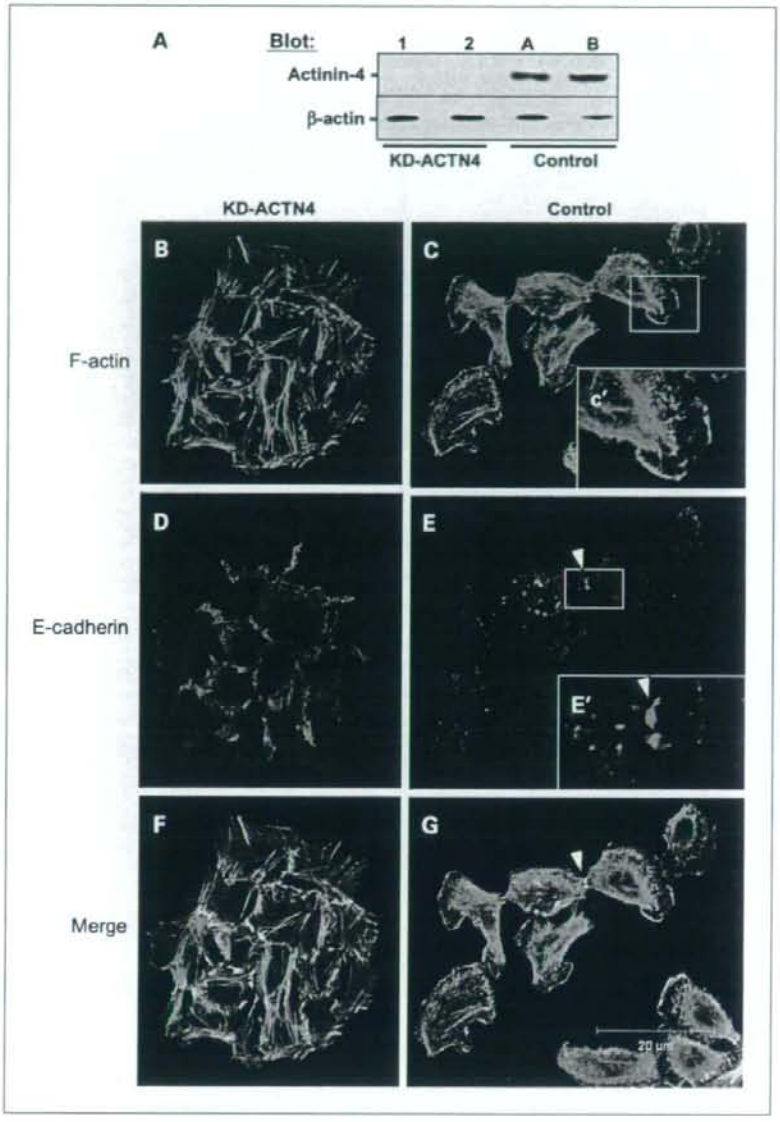

Fig. 4. Knockdown of actinin-4 alters cell morphology. *A*, Western blot analysis of actinin-4 and β-actin (loading control) protein expression in two stable clones in which expression of actinin-4 was knocked down by short hairpin RNA transfection (*KD-ACTN4*, *1* and *2*) and two control clones (*Control*, *A* and *B*). *B-G*, immunofluorescence microscopic analysis of the actin cytoskeleton (*B*, *C*, and *green* in *F* and *G*) and E-cadherin expression (*D*, *E*, and *red* in *F* and *G*) in *ACTN4* knockdown (*KD-ACTN4*; *B*, *D*, and *F*) and control (*Control*; *C*, *E*, and *G*) cells. Filamentous actin (*F-actin*) was visualized by Alexa Fluor 488 phalloidin staining. *C'* and *E'*, insets from *C* and *E*, respectively. Arrowheads, intercellular connection (*E* and *G*).

followed by the presence of lymph node metastasis (P = 0.0073; hazard ratio, 1.96; 95% confidence interval, 1.20-3.19) and distant organ metastasis (P = 0.0050; hazard ratio, 1.73; 95% confidence interval, 1.18-2.54).

Gene amplification of ACTN4 in pancreatic cancer. Recurrent amplification of the chromosome 19q13 locus containing the *AKT2* gene has been reported in the pancreatic cancer cell line Panc-1. We investigated whether the *ACTN4* gene was included within the amplicon. Fluorescence *in situ* hybridization revealed an average of 13.7 *ACTN4* (Fig. 3A) and 27.0 *AKT2* (Fig. 3B) fluorescence signals per interphase Panc-1 cell. Consistently, real-time PCR showed that the copy numbers of the *ACTN4* and *AKT2* genes were increased 6-fold and 20-fold, respectively, in comparison with the immortalized near-diploid pancreatic ductal cell line H6C7 (Supplementary Fig. S2).

Fluorescence *in situ* hybridization was then done in surgical specimens of 46 randomly selected pancreatic cancers with positive expression of actinin-4 (n = 29) and negative expression of actinin-4 (n = 17; Fig. 3C-F). There was a significant difference in the frequency of *ACTN4* gene amplification between actinin-4 expression-positive and expression-negative cases (P = 0.017, χ^2 test), when gene amplification was defined as average fluorescence signals of >4 in 20 interphase tumor cell nuclei: 11 of 29 actinin-4 expression-positive cases (37.9%; gray columns; Fig. 3G) but only 1 of 17 expression-negative cases (5.9%; unshaded columns; Fig. 3G) showed gene amplification of *ACTN4*.

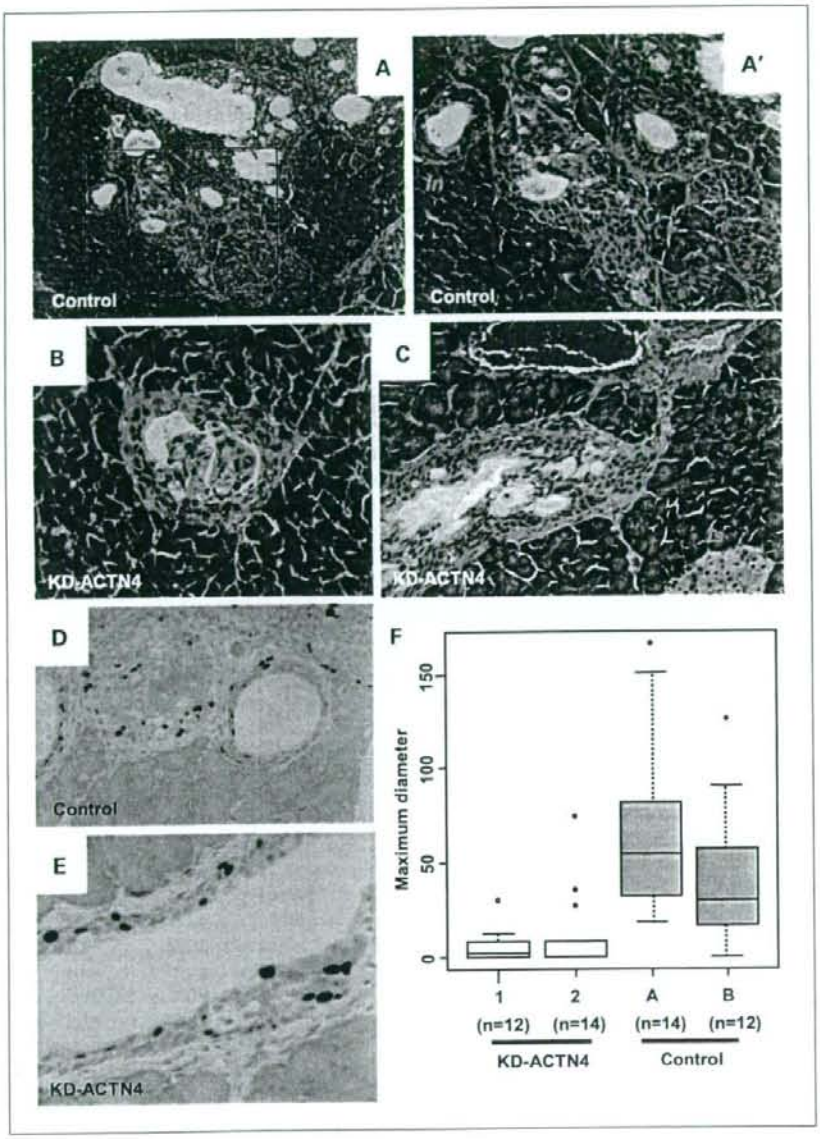

Fig. 5. Suppression of invasive growth by knockdown of actinin-4. *A-E*, H&E (*A-C*) and immunoperoxidase staining with anti-Ki67 antibody (*D* and *E*) of tumors generated by orthotopic implantation of *ACTN4* knockdown (*KD-ACTN4*; *B*, *C*, and *E*) and control (*Control*; *A* and *D*) cells into the pancreas of severe combined immunodeficiency mice. *A'*, inset in *A*. In, intraductal spreading; Du, normal pancreatic duct; Is, islet. *F*, whisker box-plot of maximum diameters (in 10^{-1} mm) of tumors generated by orthotopic implantation of *ACTN4* knockdown (*KD-ACTN4*, *1* and *2*) and control (*Control*, *A* and *B*) clones into the pancreas of severe combined immunodeficiency mice. There were significant differences between *ACTN4* knockdown and control clones ($P < 0.0001$ between KD-ACTN4-1 and Control A, $P = 0.0001$ between KD-ACTN4-2 and Control A, $P = 0.0024$ between KD-ACTN4-1 and Control B, and $P = 0.0071$ between KD-ACTN4-2 and Control B; Wilcoxon rank sum test).

Knockdown of ACTN4 expression. In order to examine the involvement of actinin-4 in the invasive growth of pancreatic cancer cells *in vivo*, we established, from the pancreatic cancer cell line BxPC3, two stable clones whose expression of actinin-4 had been knocked down by short hairpin RNA transfection (KD-ACTN4, lanes 1 and 2) and two control (nonsilencing) clones (Control, lanes A and B). We have previously reported that transient knockdown of actinin-4 expression by small interfering RNA significantly reduces the motility of BxPC3 cells in an *in vitro* migration assay (27). Western blot analysis confirmed the down-regulation of actinin-4 protein expression in the two knockdown clones (lanes 1 and 2; Fig. 4A), but not in the control clones (lanes A and B).

Knockdown of actinin-4 expression resulted in the alteration of cell shape and distribution of the actin cytoskeleton (Fig. 4B-G). Control cells were poorly connected, and filamentous actin was concentrated at the cell periphery (lamellipodia; Fig. 4C). Conversely, KD-ACTN4 cells showed tight intercellular connections, and marked extension of actin stress fibers along cellular long axes was observed (Fig. 4B). Actinin-4 competes with E-cadherin for binding to β-catenin (27). Knockdown of *ACTN4* may have restored the cell adhesion function of E-cadherin (Fig. 4D).

Scanning electron microscopy revealed the development of numerous microvilli on the dorsal surface of control cells (Control, Supplementary Fig. S3), whereas microvilli were

poorly developed in KD-ACTN4 cells (KD-ACTN4, Supplementary Fig. S3). Knockdown of actinin-4 expression reduced cell migratory activity (Supplementary Fig. S4).

Suppression of invasive growth by knockdown of actinin-4. Supplementary Fig. S5 illustrates the growth kinetics of KD-ACTN4 and control cells. KD-ACTN4 cells showed modest reduction of cell proliferation *in vitro*. However, the growth of KD-ACTN4 cells transplanted orthotopically into the pancreas of severe combined immunodeficiency mice was markedly suppressed (Fig. 5). Control cells formed masses at the sites of injection, destroying the parenchyma of the pancreas (Control; Fig. 5A) and spreading along the pancreatic ducts (*In*; Fig. 5A'). In contrast, KD-ACTN4 cells formed small nests in the connective tissue surrounding the pancreas (data not shown) or spread along the pancreatic ducts (KD-ACTN4; Fig. 5B and C). There were significant differences between the diameters of tumors generated by KD-ACTN4 clones and by control clones (Fig. 5F). However, Ki67 labeling revealed no apparent difference in cell proliferation activity between tumors generated by KD-ACTN4 and by control cells (Fig. 5D and E), consistent with the *in vitro* cell growth kinetics (Supplementary Fig. S5).

Discussion

Although the molecular mechanisms causing cancer invasion and metastasis are highly complicated, the acquisition of enhanced motility by cancer cells is a prerequisite. During the process of cell movement, actinin-4 protein levels are increased and highly concentrated at the leading edge of motile cells (4). We recently showed that increased expression of actinin-4 significantly enhances cell motility and mediates invasive growth and lymph node metastasis by colorectal cancer (6). In this study, actinin-4 was found to be overexpressed in the majority of invasive ductal carcinomas of the pancreas (Fig. 1), and increased expression of actinin-4 protein was significantly correlated with poor prognosis of patients with pancreatic cancer (Fig. 2). Knockdown of actinin-4 expression enhanced intercellular connections (Fig. 4) and significantly reduced the motility of a highly motile pancreatic cancer cell line (Supplementary Fig. S4; ref. 27). These observations lead us to conclude that actinin-4 plays a biologically significant role in pancreatic carcinogenesis.

We showed that gene amplification may underlie the increased expression of actinin-4 protein. Gene amplification of *ACTN4* was significantly more frequent in cases with increased expression of actinin-4 (Fig. 3G). However, several cases with increased expression of actinin-4 had a normal copy number of the *ACTN4* gene, and other molecular mechanisms could not be excluded. An invasive growth pattern seems to be an intrinsic feature of pancreatic cancer, and it is reasonable to assume that *ACTN4* is the target of the 19q13 amplification. Nevertheless, because several other candidate genes have been isolated from the chromosome region (16, 28, 29), the *ACTN4* gene may not be the sole target.

Recently, a familial pancreatic cancer gene on 4q32-34 was identified as *PALLD*, which encodes the protein palladin (30), another component of the actin-containing microfilaments that control cell shape, adhesion, and movement. Palladin binds to actinin and functions as a scaffold of the actin cytoskeleton (30, 31). The missense mutation of *PALLD* in the affected family was mapped to the actinin-binding domain of palladin (31). Transfection of the mutant palladin cDNA impaired the organization of the actin cytoskeleton and increased cell motility. Palladin mRNA was overexpressed in precancerous ductal dysplasia and carcinoma of the pancreas. Thus, *PALLD* mutation and palladin overexpression may have something to do with the functions of actinin-4.

Thus far, two non-muscle actinin isoforms, actinin-1 and actinin-4, have been identified. Enhanced actin stress fiber formation in KD-ACTN cells (Fig. 4B) may reflect a shift of filamentous actin from actinin-4 to actinin-1. A germ line mutation in the *ACTN4* gene is responsible for familial focal segmental glomerulosclerosis (32). Mice deficient in the *Actn4* gene manifest severe glomerular dysfunction (33), and failure of foot process extension by glomerular podocytes is thought be the major cause of focal segmental glomerulosclerosis. Knockdown of *ACTN4* in pancreatic cancer cells inhibited the formation of microvilli (Supplementary Fig. S3), probably through the same mechanism. Actinin-4 seems to be essential for the invasive growth of pancreatic cancer and may represent a candidate drug target. However, because of the lack of redundancy with actinin-1 in glomerular function, renal side effects may be a concern for therapeutics targeting actinin-4.

Actinin-4 is a multifunctional protein whose functional role is determined by partner proteins that form complexes with it. As well as the cell adhesion and cytoskeleton proteins, actinin-4 (or an unspecified non-muscle actinin) has been reported to interact with molecules of various functions, including BERP (34), Na^+/H^+ exchanger 3 (35), DNaseY (36), ATK1 (37), plasminogen activator inhibitor type-1 (38), histone deacetylase 7 (39), androgen receptor (40), and HER2/Neu/ErbB2 (41). For example, actinin-4 physically interacts with AKT1, and knockdown of *ACTN4* has been reported to inhibit the phosphorylation and nuclear translocation of AKT1. The AKT signaling pathway is known to be involved in regulating a variety of biological processes such as cell survival, proliferation, and motility (42).

In summary, we have identified increased expression and gene amplification of actinin-4 in pancreatic ductal carcinoma and clarified its clinical and biological significance. We believe that the findings reported here provide novel insights into diagnostic and therapeutic approaches to this devastating disease.

Disclosure of Potential Conflicts of Interest

No potential conflicts of interest were disclosed.

References

1. Landis SH, Murray T, Bolden S, Wingo PA. Cancer statistics, 1999. CA Cancer J Clin 1999;49:8–31.
2. Nitecki SS, Sarr MG, Colby TV, van Heerden JA. Long-term survival after resection for ductal adenocarcinoma of the pancreas. Is it really improving? Ann Surg 1995;221:59–66.
3. Lowenfels AB, Maisonneuve P. Epidemiology and prevention of pancreatic cancer. Jpn J Clin Oncol 2004;34:238–44.

4. Honda K, Yamada T, Endo R, et al. Actinin-4, a novel actin-bundling protein associated with cell motility and cancer invasion. J Cell Biol 1998;140:1383–93.
5. Yamagata N, Shyr Y, Yanagisawa K, et al. A training-testing approach to the molecular classification of resected non-small cell lung cancer. Clin Cancer Res 2003;9:4695–704.
6. Honda K, Yamada T, Hayashida Y, et al. Actinin-4 increases cell motility and promotes lymph node metastasis of colorectal cancer. Gastroenterology 2005; 128:51–62.
7. Furukawa T, Sunamura M, Horii A. Molecular mechanisms of pancreatic carcinogenesis. Cancer Sci 2006; 97:1–7.
8. Almoguera C, Shibata D, Forrester K, Martin J, Arnheim N, Perucho M. Most human carcinomas of the exocrine pancreas contain mutant c-K-ras genes. Cell 1988;53:549–54.
9. Hingorani SR, Petricoin EF, Maitra A, et al. Preinvasive and invasive ductal pancreatic cancer and its early detection in the mouse. Cancer Cell 2003;4:437–50.
10. Olive KP, Tuveson DA. The use of targeted mouse models for preclinical testing of novel cancer therapeutics. Clin Cancer Res 2006;12:5277–87.
11. Miwa W, Yasuda J, Murakami Y, et al. Isolation of DNA sequences amplified at chromosome 19q13.1-q13.2 including the AKT2 locus in human pancreatic cancer. Biochem Biophys Res Commun 1996;225: 968–74.
12. Hoglund M, Gorunova L, Andren-Sandberg A, Dawiskiba S, Mitelman F, Johansson B. Cytogenetic and fluorescence *in situ* hybridization analyses of chromosome 19 aberrations in pancreatic carcinomas: frequent loss of 19p13.3 and gain of 19q13.1-13.2. Genes Chromosomes Cancer 1998;21:8–16.
13. Mahlamaki EH, Kauraniemi P, Monni O, Wolf M, Hautaniemi S, Kallioniemi A. High-resolution genomic and expression profiling reveals 105 putative amplification target genes in pancreatic cancer. Neoplasia 2004;6:432–9.
14. Cheng JQ, Ruggeri B, Klein WM, et al. Amplification of AKT2 in human pancreatic cells and inhibition of AKT2 expression and tumorigenicity by antisense RNA. Proc Natl Acad Sci U S A 1996;93:3636–41.
15. Ruggeri BA, Huang L, Wood M, Cheng JQ, Testa JR. Amplification and overexpression of the AKT2 oncogene in a subset of human pancreatic ductal adenocarcinomas. Mol Carcinog 1998;21:81–6.
16. Kuuselo R, Savinainen K, Azorsa DO, et al. Intersex-like (IXL) is a cell survival regulator in pancreatic cancer with 19q13 amplification. Cancer Res 2007;67: 1943–9.
17. Shinoda Y, Kozaki K, Imoto I, et al. Association of KLK5 overexpression with invasiveness of urinary bladder carcinoma cells. Cancer Sci 2007;98: 1078–86.
18. Sobin L, Witteknd C. TNM classification of malignant tumors. 6th ed. New York: Wiley-Liss; 2002.
19. Japan Pancreas Society. Classification of pancreatic carcinoma. 2nd English ed., Tokyo: Kanehara & Co.; 2003.
20. Seike M, Kondo T, Mori Y, et al. Proteomic analysis of intestinal epithelial cells expressing stabilized β-catenin. Cancer Res 2003;63:4641–7.
21. Shimoyama Y, Hirohashi S, Hirano S, et al. Cadherin cell-adhesion molecules in human epithelial tissues and carcinomas. Cancer Res 1989;49:2128–33.
22. Yamada T, Takaoka AS, Naishiro Y, et al. Transactivation of the multidrug resistance 1 gene by T-cell factor 4/β-catenin complex in early colorectal carcinogenesis. Cancer Res 2000;60:4761–6.
23. Sato S, Idogawa M, Honda K, et al. β-Catenin interacts with the FUS proto-oncogene product and regulates pre-mRNA splicing. Gastroenterology 2005;129:1225–36.
24. Tsuda H, Akiyama F, Terasaki H, et al. Detection of HER-2/neu (c-erb B-2) DNA amplification in primary breast carcinoma. Interobserver reproducibility and correlation with immunohistochemical HER-2 overexpression. Cancer 2001;92:2965–74.
25. Honda K, Yamada T, Seike M, et al. Alternative splice variant of actinin-4 in small cell lung cancer. Oncogene 2004;23:5257–62.
26. Loukopoulos P, Kanetaka K, Takamura M, Shibata T, Sakamoto M, Hirohashi S. Orthotopic transplantation models of pancreatic adenocarcinoma derived from cell lines and primary tumors and displaying varying metastatic activity. Pancreas 2004;29:193–203.
27. Hayashida Y, Honda K, Idogawa M, et al. E-cadherin regulates the association between β-catenin and actinin-4. Cancer Res 2005;65:8836–45.
28. Moniaux N, Nemos C, Schmied BM, et al. The human homologue of the RNA polymerase II-associated factor 1 (hPaf1), localized on the 19q13 amplicon, is associated with tumorigenesis. Oncogene 2006;25: 3247–57.
29. Huntsman DG, Chin SF, Muleris M, et al. MLL2, the second human homolog of the Drosophila trithorax gene, maps to 19q13.1 and is amplified in solid tumor cell lines. Oncogene 1999;18:7975–84.
30. Pogue-Geile KL, Chen R, Bronner MP, et al. Palladin mutation causes familial pancreatic cancer and suggests a new cancer mechanism. PLoS Med 2006;3: e516.
31. Ronty M, Taivainen A, Moza M, Otey CA, Carpen O. Molecular analysis of the interaction between palladin and α-actinin. FEBS Lett 2004;566:30–4.
32. Kaplan JM, Kim SH, North KN, et al. Mutations in ACTN4, encoding α-actinin-4, cause familial focal segmental glomerulosclerosis. Nat Genet 2000;24: 251–6.
33. Kos CH, Le TC, Sinha S, et al. Mice deficient in α-actinin-4 have severe glomerular disease. J Clin Invest 2003;111:1683–90.
34. El-Husseini AE, Kwasnicka D, Yamada T, Hirohashi S, Vincent SR. BERP, a novel ring finger protein, binds to α-actinin-4. Biochem Biophys Res Commun 2000; 267:906–11.
35. Kim JH, Lee-Kwon W, Park JB, Ryu SH, Yun CH, Donowitz M. Ca(2+)-dependent inhibition of Na+/H+ exchanger 3 (NHE3) requires an NHE3-3KARP-α-actinin-4 complex for oligomerization and endocytosis. J Biol Chem 2002;277:23714–24.
36. Liu QY, Lei JX, LeBlanc J, et al. Regulation of DNaseY activity by actinin-α4 during apoptosis. Cell Death Differ 2004;11:645–54.
37. Ding Z, Liang J, Lu Y, et al. A retrovirus-based protein complementation assay screen reveals functional AKT1-binding partners. Proc Natl Acad Sci U S A 2006;103:15014–9.
38. Magdolen U, Schroeck F, Creutzburg S, Schmitt M, Magdolen V. Non-muscle α-actinin-4 interacts with plasminogen activator inhibitor type-1 (PAI-1). Biol Chem 2004;385:801–8.
39. Chakraborty S, Reineke EL, Lam M, et al. α-Actinin 4 potentiates myocyte enhancer factor-2 transcription activity by antagonizing histone deacetylase 7. J Biol Chem 2006;281:35070–80.
40. Jasavala R, Martinez H, Thumar J, et al. Identification of putative androgen receptor interaction protein modules: cytoskeleton and endosomes modulate androgen receptor signaling in prostate cancer cells. Mol Cell Proteomics 2007;6:252–71.
41. Wang SE, Shin I, Wu FY, Friedman DB, Arteaga CL. HER2/Neu (ErbB2) signaling to Rac1-1 is temporally and spatially modulated by transforming growth factor β. Cancer Res 2006;66:9591–600.
42. Testa JR, Bellacosa A. AKT plays a central role in tumorigenesis. Proc Natl Acad Sci U S A 2001;98: 10983–5.

Preoperative Evaluation of Invasive and Noninvasive Intraductal Papillary-Mucinous Neoplasms of the Pancreas

Clinical, Radiological, and Pathological Analysis of 123 Cases

Satoshi Nara, MD, Hiroaki Onaya, MD, PhD,† Nobuyoshi Hiraoka, MD, PhD,‡ Kazuaki Shimada, MD, PhD,* Tsuyoshi Sano, MD, PhD,§ Yoshihiro Sakamoto, MD, PhD,* Minoru Esaki, MD, PhD,* and Tomoo Kosuge, MD, PhD**

Objective: We aimed to investigate preoperative findings that are useful to distinguish intraductal papillary-mucinous neoplasm (IPMN) subtypes.

Methods: One hundred twenty-three patients who underwent pancreatectomy for IPMN were analyzed clinicopathologically and radiologically. Invasive IPM carcinomas (IPMCs) were subdivided into early-stage nonaggressive (minimally invasive IPMC [MI-IPMC]) and more advanced and aggressive (invasive carcinoma originating in IPMC [IC-IPMC]) subtypes according to our recently proposed pathological criteria.

Results: The lesions consisted of 27 IPMNs with low-grade dysplasia, 14 IPMNs with moderate dysplasia, 21 IPMNs with high-grade dysplasia, 30 MI-IPMCs, and 31 IC-IPMCs. Multidetector-row computed tomography detected a component of invasive carcinoma in IC-IPMC with 86% sensitivity and 100% specificity. In patients with IPMNs other than IC-IPMC, multivariate analysis demonstrated 3 significant predictive factors of malignancy: IPMN size (>40 mm), IPMN duct type (main pancreatic duct or mixed type), and the presence of a mural nodule or thick septum. The diagnostic score obtained using these 3 factors showed a strong correlation with the presence of malignancy.

Conclusions: For preoperative evaluation of patients with IPMN, it is recommended to rule out IC-IPMC using multidetector-row computed tomography and then to categorize IPMN other than IC-IPMC according to malignant potential based on the diagnostic score.

Key Words: intraductal papillary-mucinous neoplasm, pancreas, minimal invasion, diagnostic score, prognostic factor

(*Pancreas* 2009;38: 8–16)

Intraductal papillary-mucinous neoplasm (IPMN) of the pancreas is a well-characterized entity both clinically and pathologically. IPMNs are characterized by intraductal proliferation of neoplastic mucinous cells, which usually form papillae and lead to cystic dilation of the pancreatic ducts, forming a clinically and macroscopically detectable mass.[1,2] IPMNs include a wide spectrum of tumors that vary in their malignant potential. It is highly speculated that IPMN progresses from low-grade, moderate, and high-grade dysplasia (carcinoma in situ [CIS]) to invasive IPM carcinoma (IPMC) and eventually to invasive adenocarcinoma.[1–5] Depending on the grade of IPMN during the progression from noninvasive IPMN to invasive IPMC, the choice of treatment varies from a conservative approach to radical pancreatectomy with lymph node (LN) dissection.[6] Therefore, it is very important to determine the subtype of IPMN accurately before surgery to optimize the therapy.

Preoperative distinction of IPMN subtypes is not easy, even when multiple modalities are used.[7] It is necessary to inspect the entire lesion because various tumor grades are usually present in 1 lesion; however, this is problematic to perform directly and biopsy of the lesion is difficult because IPMNs are located in the pancreas and often shows cystic features. Some groups reported the high accuracy of pancreas juice cytology[8] or peroral intraductal pancreatoscopy,[9] but these procedures require expertise and are not free from complications; thus, routine practice of these modalities remains limited.

Previous studies have proposed some factors that are predictive of IPMN malignancy, such as the presence of symptoms (particularly jaundice), positive pancreatic juice cytology, tumor size greater than 30 to 50 mm, main pancreatic duct (MPD) type or mixed type, dilatation of MPD, the presence of a mural nodule, papillary projection, a thick septum, and wall thickening.[7,8,10–12] Except for the former two, these features can be observed by radiological examination, but these factors are not always related to the malignancy, and none of them can be used alone.

Another problem is that no unequivocal pathological criteria for distinguishing invasive IPMC have been established. The recent consensus is that the malignant potential of IPMN is dependent on the presence of invasive cancer and its extent.[13–19] However, invasive IPMC categorized by the Armed Forces Institute of Pathology (AFIP) and World Health Organization classifications[1,2] covers cancer with variable biological behavior, with the 5-year survival rate varying substantially between 24% and 60%.[13–19] Therefore, invasive IPMC should be regarded separately as either aggressive or nonaggressive. The classification of the Japan Pancreas Society subdivides invasive IPMC into minimally invasive IPMC (MI-IPMC) and invasive carcinoma originating in IPMC (IC-IPMC) (Fig. 1).[20] Minimally invasive IPMC represents invasive IPMC with early-stage nonaggressive characteristics, whereas IC-IPMC represents a more advanced tumor. Minimally invasive IPMC has been reported to have a better surgical outcome than IC-IPMC,[21,22] although the criteria used for defining MI-IPMC are still unclear.[20] Recently, we

From the *Hepatobiliary and Pancreatic Surgery Division and †Diagnostic Radiology Division, National Cancer Center Hospital; and ‡Pathology Division, National Cancer Center Research Institute, Tokyo; and §Hepatobiliary and Pancreatic Surgery Division, Aichi Cancer Center Hospital, Nagoya, Japan.

Received December 3, 2007.
Accepted for publication May 15, 2008.

Reprints: Satoshi Nara, MD, Hepatobiliary and Pancreatic Surgery Division, National Cancer Center Hospital, 5-1-1 Tsukiji, Chuo-ku, Tokyo 104-0045, Japan (e-mail: sanara@ncc.go.jp).

The authors have no direct or indirect commercial or financial incentives associated with publishing this article.

This work was supported by a Grant-in-Aid for Third Term Comprehensive 10-Year Strategy for Cancer Control from the Ministry of Health, Labor and Welfare of Japan and a Grant-in-Aid for Scientific Research from the Ministry of Education, Culture, Sports, Science and Technology of Japan.

ISSN: 0885-3177
DOI: 10.1097/MPA.0b013e318181b90d

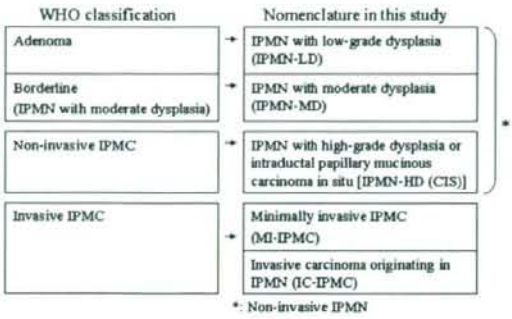

FIGURE 1. The nomenclature of IPMN used in this study is based on AFIP classification[1] and corresponded to the World Health Organization classification.[2] Invasive IPMCs are further divided into MI-IPMC and IC-IPMC according to our diagnostic criteria,[23] which is based on the classification of the Japan Pancreas Society.[20]

proposed simple and practical diagnostic criteria for MI-IPMC[23] and used them to classify IPMN in 104 patients. Those with MI-IPMC showed a good outcome similar to that of noninvasive IPMN after curative resection, whereas patients with IC-IPMC showed a worse outcome similar to that of conventional ductal carcinoma of the pancreas. In addition, IC-IPMCs were frequently associated with LN metastasis, necessitating LN dissection during operation, whereas no LN metastasis was observed among patients with MI-IPMCs.[22,23] Thus, precise discrimination between MI-IPMC and IC-IPMC is important not only for predicting the postoperative outcome, but also for deciding the operative procedure.

In the present retrospective study, we examined 123 patients with IPMN and assessed their clinical and radiological findings for preoperative prediction of IPMN pathological subtypes.

MATERIALS AND METHODS

Study Population

This study was approved by the ethics committee of the National Cancer Center, Japan. Between January 1984 and December 2006, a total of 123 patients underwent pancreatectomy for IPMN at the National Cancer Center Hospital, Japan. Seventy-eight (63%) of the surgical operations were performed after January 2001. Eight patients who also had ductal carcinoma of the pancreas that was not directly associated with IPMN were excluded from the study. The study patients are composed of 70 men and 53 women aged 40 to 84 years (mean, 64.7 years). Upon pathological examination, 5 patients were found to have multiple IPMNs in the resected specimen. We chose 1 lesion with the highest grade, then the largest lesion among multiple IPMNs, and used it for this study. Clinical data and characteristics of the IPMNs are summarized in Table 1. Every patient was followed up in the outpatient clinic every 1 to 3 months during the first postoperative year, and every 6 to 12 months thereafter. No patient was lost to follow-up. Clinical and laboratory data for every patient were obtained from the medical records.

Pathological Examination

All of the IPMNs were pathologically reexamined, and the diagnosis of IPMN was confirmed. Surgically resected specimens were fixed in 10% formalin and cut into serial 5-mm-thick slices, horizontally in the pancreas head and sagittally in the

TABLE 1. Demography of Patients With IPMNs

Pathological Diagnosis	IPMN-LD or IPMN-MD (n = 41)	IPMN-HD (CIS) (n = 21)	MI-IPMC (n = 30)	IC-IPMC (n = 31)	Total (n = 123)	*P*
Mean age, yrs	64.1 ± 8.0	62.0 ± 9.6	64.9 ± 8.6	67.4 ± 10.4	64.7 ± 9.1	0.186
Median age (range), yrs	65 (42–77)	60 (40–80)	66 (41–76)	69 (45–84)	66 (40–84)	
Male, %	25 (61.0%)	10 (47.6%)	19 (63.3%)	16 (51.6%)	70 (56.9%)	0.599
Chief complaints						0.024*
Complaints (−)	27	13	15	12	67	
Complaints (+)	14	8	15	19	56	
Radiological findings						
Tumor location						0.005
Ph included	29	15	22	12	78	
Ph excluded	12	6	8	15	41	
Total pancreas (diffuse)	0	0	0	4	4	
rIPMN size, mm	35.7 ± 16.2	44.5 ± 17.4	53.6 ± 31.6	48.4 ± 30.1	44.8 ± 25.4 (10–136)	0.022
rMPD diameter, mm	4.5 ± 2.8	6.5 ± 4.8	10.7 ± 6.6	6.4 ± 4.5	6.9 ± 5.2 (1–31)	<0.001
rIPMN type						<0.001
rMPD type	0	5	11	10	26	
rBD type	33	12	6	8	59	
rMixed type	8	4	13	13	38	
Mural nodule (>3 mm), %	10 (24%)	15 (71%)	20 (67%)	15 (48%)	60 (49%)	<0.001
Thick septum (>2 mm), %	11 (27%)	8 (38%)	14 (47%)	13 (42%)	46 (37%)	0.343
Size of invasive cancer, mm	—	—	<5	36.1 ± 17.7 (6–90)	—	

*Comparison between noninvasive IPMN and invasive IPMN (MI-IPMC + IC-IPMC) by χ^2 test.

Ph indicates pancreas head; rIPMN size, IPMN size measured on CT; rIPMN type, IPMN type determined based on CT findings.

pancreas body and tail. All the sections were stained with hematoxylin and eosin for pathological examination. After histopathological examination of all the sections, the lesion was classified as IPMN with low-grade dysplasia (IPMN-LD), moderate dysplasia (IPMN-MD), high-grade dysplasia (IPMN-HD; CIS), or invasive IPMC according to the AFIP classification.[1] The lesion was graded by the highest degree of atypia. Invasive IPMCs were further divided into MI-IPMC or IC-IPMC according to our proposed criteria.[23] We classified the invasive features of IPMC into 3 patterns: infiltrative growth, mucous rupture, and expansive growth. *Infiltrative growth* is an invasive pattern commonly seen in conventional ductal carcinoma of the pancreas, showing tubular or mucinous invasion. On the other hand, mucous rupture and expansive growth are unique features of IPMC, which grows expansively with large amounts of mucus secretion. *Mucous rupture* refers to mucous lakes around an intraductal IPMC, sometimes containing scanty floating cancer cells, formed by rupture of pancreatic ducts through intraductal high pressure. *Expansive growth* refers to the loss of the basement membrane because of marked dilatation of pancreatic duct, sometimes resulting in the involvement (erosion or fistula formation) of the bowel wall or major vessels. We defined *minimal invasion* as (*a*) an infiltrative growth of 5 mm or less, (*b*) mucous rupture not associated with infiltrative growth of more than 5 mm, or (*c*) expansive growth without fistula formation with major vessels. And when at least 1 feature beyond the previously mentioned criteria of minimal invasion was present, the lesion was diagnosed as IC-IPMC. Invasive carcinoma originating in IPMC was originally defined as a lesion consisting of IPMN and invasive carcinoma with predominance of the IPMN component.[20] This type of invasive carcinoma shows continuous transition between invasive carcinoma and intraductal IPMC. In this study, we also included a new group in which invasive carcinoma apparently originated from IPMN but was predominant over the IPMN component because there was no statistically significant survival difference between IC-IPMCs with predominant IPMN component and IC-IPMCs with predominant invasive cancer component in our preliminary analysis.

The measured size of an IPMN (excluding the invasive component) was denoted as the *pIPMN size*, defined as the maximum diameter of microscopically recognized noninvasive IPMN. The size of invasive cancer was measured separately in patients with MI-IPMC and IC-IPMC. The duct type of IPMN was also determined according to where the IPMN was mainly present. When the IPMN was located mainly in the MPD and extended to a small region of the branch duct (BD) (length, <1 cm), it was defined as the MPD type. When the IPMN located mainly in the BD and extended to a small region of the

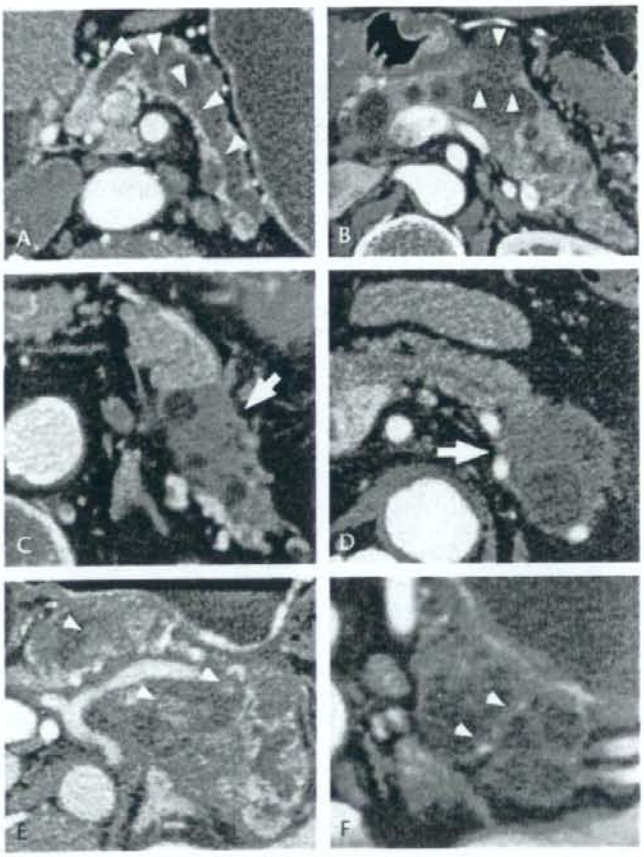

FIGURE 2. A and B, MDCT images show papillary projections in the dilated pancreatic ducts (arrowheads). Papillary projections appear as subtle brushlike low attenuations along the wall of the pancreatic ducts, reflecting the extent of IPMN. C and D, MDCT images of IC-IPMCs. The invasive cancer components (arrows) are depicted as areas of low attenuation adjacent to or surrounding the cystic IPMN lesions. The retropancreatic invasion adjacent to the splenic artery is shown (arrow) (D). E and F, MDCT images showing mural nodules (E) and thick septa (F). E, Various-sized mural nodules are evident in the intraductal carcinoma component (arrowheads). F, The thick septum is indicated by arrowheads in noninvasive IPMCs.

MPD (length, <1 cm), it was defined as the BD type; otherwise, the IPMN was defined as the mixed type.

Radiological Examination

All 123 patients underwent contrast-enhanced computed tomography (CT) and extracorporeal ultrasonography (US) examinations, whereas magnetic resonance cholangiopancreatography (MRCP) was performed in 77 patients (63%). As endoscopic retrograde cholangiopancreatography and endoscopic US are not routinely performed at our institution, data for both examinations were excluded from the present analysis. The CT images were obtained using single-slice helical CT machines before 2000, and thereafter using multidetector-row CT (MDCT) with a 1- to 2-mm section thickness. Of the 123 patients, 71 (58%) underwent MDCT examinations.

The CT images were retrospectively reviewed independently by 2 investigators (S.N. and H.O.) without knowledge of the pathological diagnosis. Discrepancy was less than 5%, and cases with disagreement were resolved by discussion. The size of the IPMN (designated as rIPMN size), the duct type

TABLE 2. Univariate Analysis of Preoperative (Clinical or Radiological) Findings Associated With Subtypes of IPMNs

Variables	(1) IPMN-LD or IPMN-MD (n = 41)	(2) IPMN-HD (CIS) (n = 21)	(3) MI-IPMC (n = 30)	(4) IC-IPMC (n = 31)	Total (n = 123)	P (χ^2 or Fisher Exact Test) (2) (3) vs (4)	(1) vs (2) (3)	(2) vs (3)
Sex						0.643	0.690	0.265
Male	25	10	19	16	70			
Female	16	11	11	15	53			
Age, yrs						0.020	0.858	0.969
≤70	32	16	23	16	87			
>70	9	5	7	15	36			
Chief complaint						0.155	0.287	0.400
(−)	27	13	15	12	67			
(+)	14	8	15	19	56			
Jaundice						0.098	0.500	0.506
(−)	41	21	28	26	116			
(+)	0	0	2	5	7			
CEA, ng/mL						0.288	0.376	0.134
≤10	40	21	26	26	113			
>10	1	0	4	5	10			
CA-19-9, U/mL						<0.001	0.296	0.119
≤37	31	20	23	10	84			
>37	10	1	7	21	39			
Radiological findings								
Detection of invasive cancer on CT*						<0.001	0.126	0.134
(−)	41	21	26	6	94			
(+)	0	0	4	25	29			
Tumor location						0.055	0.847	0.881
Ph included	29	15	22	16	82			
Ph excluded	12	6	8	15	41			
Tumor distribution						0.110	0.532	0.034
1 segment	35	20	21	20	96			
2 or 3 segments	6	1	9	11	27			
rIPMN size, mm						0.321	<0.001	0.917
≤40	31	8	11	15	65			
>40	10	13	19	16	58			
rMPD diameter, mm						0.120	0.005	0.020
≤8	36	17	14	24	91			
>8	5	4	16	7	32			
rIPMN duct type						0.371	<0.001	0.006
rMPD or rMixed	8	9	24	23	64			
rBD	33	12	6	8	59			
Mural nodule (>3 mm) or thick septum (>2 mm)						0.079	0.001	0.969
(−)	24	5	7	13	49			
(+)	17	16	23	18	74			

*CT images obtained using both single-slice helical CT and MDCT.

CEA indicates carcinoembryonic antigen; Ph, pancreas head.

of IPMN (designated as rIPMN duct type, and MPD, BD, and mixed type being denoted as rMPD, rBD, and rMixed type, respectively), the distribution of IPMN (head/uncus, body, or tail), and the MPD diameter (designated as rMPD diameter) were determined. The *rIPMN size* was defined as the maximum diameter of an entire noninvasive IPMN lesion, including not only the definitely cystic and/or intraductal papillary component, but also subtle papillary projections reflecting spread along the pancreatic duct (Figs. 2A, B).[24] The invasive component was excluded from the measurement of rIPMN size. The size of invasive component was measured separately depending on the CT findings. The presence of invasive carcinoma in patients with IC-IPMC was regarded as positive when an irregularly shaped hypoattenuating solid mass was detected adjacent to or surrounding an IPMN on contrast-enhanced CT.[25] The replacement of the pancreatic parenchyma by a hypoattenuating solid mass, proliferation into the extrapancreatic tissue, and encasement of surrounding vessels were all regarded as signs of invasion, similarly to the conventional invasive ductal carcinoma of the pancreas (Figs. 2C, D). We also assessed the presence of a mural nodule (if its size was >3 mm; Fig. 2E)[10] or a thick septum (if its size was >2 mm; Fig. 2F)[12] on image analysis including CT, US, and MRCP, if available.

Statistical Analysis

Continuous data were presented as mean ± SD. The cutoff values for rIPMN and pIPMN size for differentiating benign and malignant lesions were investigated by constructing receiver operating characteristic (ROC) curves. Differences between categorical variables were evaluated using χ^2 test or Fisher exact test. One-way analysis of variance was used to compare the means of 3 or more groups. Significant predictors in the univariate analysis were included in a backward stepwise logistic regression model for multivariate analysis. Differences at $P < 0.05$ were considered statistically significant. Statistical analyses were performed using SPSS 11.0J software (SPSS Inc, Chicago, Ill).

RESULTS

Postoperative pathological examination revealed that the studied lesions are composed of 27 IPMN-LDs, 14 IPMN-MDs, 21 IPMN-HD (CIS), 30 MI-IPMCs, and 31 IC-IPMCs (Table 1). More than half of the IPMNs were discovered incidentally in asymptomatic patients during health check-up or follow-up examinations after treatment of other organ diseases, and such cases were significantly common among noninvasive IPMNs ($P = 0.024$; Table 1). Chief complaints at the initial presentation included abdominal pain (n = 28), exacerbation of diabetes mellitus (n = 9), back pain (n = 7), jaundice (n = 7), weight loss (n = 7), appetite loss (n = 4), general fatigue (n = 2), carbohydrate antigen 19-9 (CA-19-9) elevation (n = 2), vomiting (n = 1), and fever (n = 1).

TABLE 3. Multivariate Analysis of Preoperative (Clinical or Radiological) Findings Associated With Subtypes of IPMNs

	Odds Ratio (95% CI)	P*
IPMN-HD (CIS) and MI-IPMC vs IC-IPMC		
Invasive cancer detected on CT†	53.9 (14.0–208)	<0.001
CA-19-9 >37 U/mL	4.38 (1.22–15.8)	0.0024
IPMN-LD or IPMN-MD vs IPMN-HD (CIS) and MI-IPMC		
rMPD or rMixed type	4.92 (1.75–13.8)	0.003
Mural nodule or thick septum (+)	2.97 (1.08–8.14)	0.035
rIPMN size >40 mm	2.88 (1.04–8.02)	0.042
IPMN-HD (CIS) vs MI-IPMC		
rMPD or rMixed type	5.33 (1.54–18.5)	0.008

*Logistic regression analysis (backward stepwise method).
†CT images obtained using both single-slice helical CT and MDCT.

TABLE 4. Accuracy of CT Detection of Invasive Cancer in IC-IPMC

A. MDCT

	CT detection of invasive cancer		Sensitivity 86%
Pathological diagnosis	(+)	(−)	Specificity 100%
IC-IPMC (+)	18	3	21
IC-IPMC (−)	0	50	50
	18	53	71

B. Single-slice helical CT

	CT detection of invasive cancer		Sensitivity 70%
Pathological diagnosis	(+)	(−)	Specificity 90%
IC-IPMC (+)	7	3	10
IC-IPMC (−)	4	38	42
	11	41	52

Preoperative Detection of IC-IPMC

To test which preoperative (clinical and radiological) variables were closely associated with IPMN pathological subtypes, their relationship was examined (Table 2). As reported previously,[21–23,26] the postoperative outcome of patients with IC-IPMC was significantly worse than that of patients with MI-IPMC or noninvasive IPMN, and LN metastasis was exclusively associated with IC-IPMC, underlining the importance of preoperative detection of IC-IPMC for therapeutic planning. Univariate analysis showed that the following preoperative variables were closely associated with the pathological subtypes of IC-IPMC: older than 70 years, the presence of invasive cancer detected on CT (both single-slice helical CT and MDCT), and CA-19-9 greater than 37 U/mL (Table 2). Multivariate analysis showed

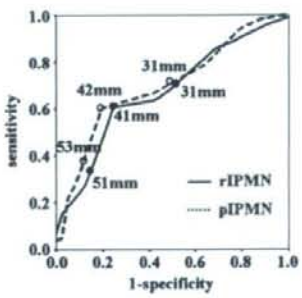

FIGURE 3. The ROC curves of rIPMN and pIPMN size. The optimal cutoff values of rIPMN and pIPMN size for detection of malignancy (carcinoma positive in a lesion) were 41 and 42 mm, respectively.

that the presence of invasive cancer detected on CT (both single-slice helical CT and MDCT) and CA-19-9 greater than 37 U/mL were significant predictive variables for IC-IPMC (Table 3).

We then analyzed how precisely CT was able to detect invasive cancers in patients with IC-IPMC. Among the 71 patients who underwent MDCT, the presence of IC-IPMC was detected with 86% sensitivity and 100% specificity, whereas single-slice helical CT (n = 52) showed 70% sensitivity and 90% specificity. Thus, the overall sensitivity and specificity of CT (n = 123) to detect invasive cancer in patients with IC-IPMC were 81% and 96%, respectively (Table 4).

Preoperative Evaluation of IPMNs Other Than IC-IPMC

We investigated the clinical and radiological findings correlated with subtypes of IPMN other than IC-IPMC (n = 92; Table 2). We excluded IC-IPMCs in which invasive cancer was not detected by CT because we aimed to clarify the characteristics of pathologically proven IPMN-HD (CIS) and MI-IPMC. Our previous study showed no significant difference in the postoperative outcome between patients with noninvasive IPMN and MI-IPMC, although 2 of 26 patients with MI-IPMC experienced recurrence.[23] Other groups also reported that 2 of 17 patients with noninvasive IPMC (IPMN-HD [CIS]) had recurrent invasive carcinoma,[13] and that 1 of 14 patients with noninvasive IPMC (IPMN-HD [CIS]) and 1 of 6 patients with MI-IPMC had recurrence after surgery.[22] Thus, preoperative detection of IPMN-HD (CIS) and MI-IPMC is a clinically important consideration, as much as the detection of IC-IPMC. The optimal cutoff values of rIPMN and pIPMN size for the detection of malignancy (IPMN-HD [CIS] and MI-IPMC) were determined to be 41 and 42 mm, respectively, on the basis of the ROC curve (Fig. 3); therefore, we adopted a cutoff value of 40 mm for rIPMN size. Univariate analysis showed that the following variables were significantly associated with malignant IPMC other than IC-IPMC: rIPMN size greater than 40 mm, rMPD diameter greater than 8 mm, rMPD or rMixed type, and the presence of a mural nodule or thick septum (Table 2). Multivariate analysis showed that rIPMN size greater than 40 mm, rMPD or rMixed type, and the presence of a mural nodule or thick septum were significant predictive factors of malignancy (Table 3).

TABLE 5. Diagnostic Score and Results in Patients With IPMN Other Than IC-IPMC (n = 92)

A. Diagnostic score (the sum of acquired points)

Predictive variables	Acquired point
rMPD or rMixed type	Yes, 1; No, 0
Presence of mural nodule or thick septum	Yes, 1; No, 0
rIPMN size >40 mm	Yes, 1; No, 0

B. Comparison of diagnostic score between patients with benign IPMN (IPMN-LD and IPMN-MD) and patients with malignant IPMN (IPMN-HD [CIS] and MI-IPMC)

Score	Benign	Malignant	Total	Risk ratio of presence of carcinoma	95% CI
0	18 (86%)	3 (14%)	21	0.13	0.042–0.42
1	14 (56%)	11 (44%)	25	0.63	0.32–1.2
2	6 (25%)	18 (75%)	24	2.4	1.1–1.5
3	3 (14%)	19 (86%)	22	5.1	1.6–16.0

C. Comparison of diagnostic score between patients with noninvasive IPMN (IPMN-LD, IPMN-MD, and IPMN-HD [CIS]) and patients with MI-IPMC

Score	Noninvasive IPMN	MI-IPMC	Total	Risk ratio of presence of carcinoma	95% CI
0	20 (95%)	1 (5%)	21	0.10	0.015–0.73
1	19 (76%)	6 (24%)	25	0.65	0.29–1.5
2	15 (63%)	9 (38%)	24	1.2	0.61–2.5
3	8 (36%)	14 (64%)	22	3.6	1.7–7.7

Numbers in parentheses denote the percentage of the number in the *Total* column.

Effectiveness of Diagnostic Score for Prediction of Noninvasive IPMC and MI-IPMC

It was unlikely that any of these preoperative variables (Table 3) alone would facilitate the accurate prediction of IPMN pathological subtypes (Table 2); therefore, we tried to predict the pathological subtypes of IPMN accurately by combining 3 variables: rIPMN size, rIPMN duct type, and the presence of a mural nodule or thick septum. A diagnostic score was devised with the aim of preoperatively identifying patients at high risk for malignancy among patients with IPMN other than IC-IPMC. The score was calculated by assigning 1 point for each of rIPMN size greater than 40 mm, rMPD or rMixed type, and mural nodule or thick septum detected on preoperative images (Table 5). The rates of malignancy (ie, IPMN-HD [CIS] and MI-IPMC) were 14%, 44%, 75%, and 86% in the patient groups with diagnostic scores of 0, 1, 2, and 3, respectively. The risk ratio of carcinoma among patients with a score 2 or 3 was 3.3 (95% confidence interval [CI], 1.8–6.0).

Comparison between IPMN-HD (CIS) and MI-IPMC showed that tumor distribution in 2 or 3 segments, MPD diameter greater than 8 mm, and rMPD or rMixed type were significantly associated with MI-IPMC by univariate analysis (Table 2), and rMPD or rMixed type remained significant by multivariate analysis (Table 3). The rates of minimal invasion were 5%, 24%, 38%, and 64% in the patient groups with diagnostic scores of 0, 1, 2, and 3, respectively (Table 5). The risk ratio of minimal invasion among patients with a score of 3 was 3.6 (95% CI, 1.7–7.7).

DISCUSSION

Recent studies on the natural history of IPMNs have revealed that the prevalence of malignancy is substantially low in small (<3 cm) BD-type IPMNs without mural nodules[27] and that it takes a relatively long period until noninvasive IPMNs progress to invasive IPMCs.[28] In addition, the current consensus regarding the malignant potential of IPMN is that its aggressiveness is dependent on the presence of invasive cancer, the extent of cancer invasion, and the biological characteristics of cancer cells.[13–19] Furthermore, MI-IPMC shows nonaggressive characteristics similar to noninvasive IPMN, whereas IC-IPMC has aggressive characteristics comparable to conventional ductal carcinoma of the pancreas.[23] These findings suggest that the therapeutic strategy for IPMN ought to differ according to the grade. Conservative treatment may be possible in selected cases of early-stage noninvasive IPMN.[29] Function-preserving pancreatectomy may be a treatment option in some noninvasive IPMNs.[30] On the other hand, as IC-IPMCs are often associated with LN metastasis[22,23] (an incidence of 61% at our institution), radical pancreatectomy with LN dissection is necessary for curative resection. Therefore, it is becoming more important to

categorize IPMN preoperatively into its corresponding pathological subtypes accurately.

Here, we retrospectively studied 123 patients who underwent surgical resection of IPMN and analyzed which preoperative findings could precisely predict the pathological subtypes. We found that MDCT was able to detect the presence of invasive cancer in IC-IPMC with 86% sensitivity and 100% specificity. We also found that rIPMN size greater than 40 mm, rMPD or rMixed type, and the presence of a mural nodule or thick septum were significant predictive factors of malignancy by multivariate analysis in patients with IPMNs other than IC-IPMC. Furthermore, the diagnostic score obtained using these 3 predictive factors showed a good correlation with the presence of carcinoma.

The clinical and radiological features of IC-IPMC are substantially different from other IPMNs. The IC-IPMCs are frequently associated with high levels of serum CA-19-9, and the invasive component of IC-IPMCs is frequently visible on CT (Table 3). These features of IC-IPMC, combined with the poor postoperative prognosis and high rate of LN metastasis, indicate that we should separate IC-IPMC from other IPMNs and treat them similarly to conventional invasive ductal carcinoma of the pancreas. When IC-IPMC is present, aggressive treatment ordinarily applied to the conventional pancreatic cancer may be indicated. This is in marked contrast with the fact that LN metastasis is almost zero in noninvasive IPMC or MI-IPMCs, and function-preserving surgery could be indicated for this patient group. Thus, we think clinicians should pay more attention to detect an associated invasive carcinoma (IC-IPMC) at initial diagnosis of IPMN.

On the basis of these findings, we propose a 2-step algorithm for determining the therapeutic strategy for patients with IPMN (Fig. 4). For the first step, patients with IPMN are categorized according to whether MDCT reveals an invasive cancer (IC-IPMC) in the lesion. For the second step, patients with IPMN other than IC-IPMC are categorized according to whether the diagnostic score suggests the presence of malignancy (Table 5). The malignancy rate was significantly high (risk ratio, 3.3; $P < 0.001$) in patients with a diagnostic score of 2 or 3. Malignancy in IPMN was detected in patients with a diagnostic score of 2 or 3, with 73% sensitivity and 78% specificity; thus, these patients should be taken to an immediate surgical operation to resect the IPMN. For patients with a diagnostic score of 1, resection is advocated for low-risk patients with a reasonable life expectancy, considering that about half (44%) of this patient group had carcinoma, although the relative risk of malignancy is lower than in patients with a diagnostic score of 2 or 3. Patients with a diagnostic score of 0 had the lowest risk of malignancy (0.13 [95% CI, 0.042–0.42]). In our series, the diagnostic score of 0 indicated IPMN as a benign lesion with 44% sensitivity and 94% specificity. Combined with previous reports showing a low occurrence rate of invasive cancer in this patient group,[28,29] these findings suggest that careful nonoperative management may be applicable for selected patients, especially those who are older or have severe complications; however, it should not be ignored that 3 (14%) of 21 patients in this group harbored carcinoma (Table 5B). Thus, "wait-and-watch" management is not always recommended for patients with a diagnostic sore of 0, and conservative treatment may be applicable in selected cases with well-informed consent about the risk of malignancy. Further accumulation of patients' follow-up data on the natural history of IPMN or the emergence of new accurate molecular markers is necessary to establish more relevant criteria for the observation strategy. Currently, balancing the malignant potential of IPMN with the risk of surgery and life expectancy may be the most practical approach for determining the indication and extent of surgery.

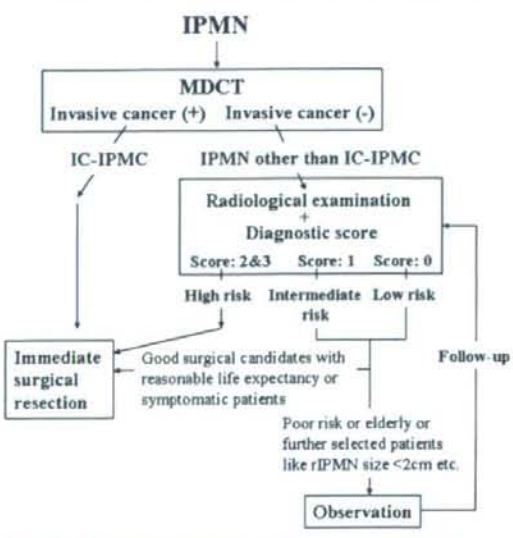

FIGURE 4. Proposed treatment algorithm for preoperative evaluation of patients with IPMN.

In this study, we were able to detect a component of invasive carcinoma in IC-IPMC using MDCT, with 86% sensitivity and 100% specificity, regardless of the size of invasive cancer. This is compatible with a recent report from another group, in which MDCT detected invasive IPMN with high sensitivity and specificity.[25] Although some authors have emphasized the diagnostic advantage of MRCP for the detection of cystic lesions,[31,32] its ability to detect solid invasive cancer associated with IPMN has not been well established. Other authors have reported that MDCT has marked ability to detect small conventional invasive cancers of the pancreas.[33,34] Although we have not yet compared the abilities of MDCT with those of MRCP for the detection of IC-IPMC, the present study has provided evidence that MDCT is very useful for the accurate detection of IC-IPMC. In our series, MDCT produced no false-positive images of patients with IC-IPMC, although it is possible that inflammatory change in the adjacent pancreatic parenchyma may be misdiagnosed as invasive cancer, as has been reported in cases of conventional invasive cancer of the pancreas.[35] Furthermore, the invasion of mucinous carcinoma may be misinterpreted as an ordinary cystic lesion without invasion.

Pathological examination revealed that IPMNs formed cystic or macroscopically papillary lesions and often spread to the surrounding pancreatic ducts. Low papillary features or spreading to minimally dilated ducts was also evident. To assess the size of IPMN on CT images, we carefully inspected the subtle signs corresponding to their features, especially papillary projection into the pancreatic duct, which has been reported to reflect the lateral spreading of low papillary lesions.[24] We examined the accuracy of radiological evaluation such as the size of rIPMN and the rIPMN duct type by comparison with pIPMN size and pIPMN duct type, respectively, using 92 IPMNs other than IC-IPMC. The size of rIPMN was measured fairly accurately and corresponded to the size of pIPMN ± 20% in 92.4% of cases and to the size of pIPMN ± 10% in 67.4% of cases. The rIPMN duct type was correctly evaluated in all but 7% of

IPMN cases. To improve the accuracy of such preoperative evaluation, additional examinations such as endoscopic retrograde cholangiopancreatography, endoscopic US, and magnetic resonance imaging may be helpful to reveal the more detailed characteristics of the lesion, if precise assessment of a laterally spreading lesion is difficult using MDCT. The discrepancy between imaging data and pathological findings may be 1 reason why intraoperative frozen-section analysis is necessary to secure a tumor-free margin.[36]

Historically, there were few reports mentioning about the radiological size of rMPD-type IPMN, and only MPD diameter has been measured.[10,17] The reason may be because the size of rMPD-type IPMN was difficult to be measured radiologically, especially those that are not macroscopically cystic and only accompanied with a diffusely dilated MPD. However, the recent advancement of radiological examinations, especially high-spatial resolution MDCT, makes it possible to evaluate the horizontal extension of intraductal epithelial lesion in the hepatobiliary-pancreatic region. For example, a high diagnostic accuracy of horizontal spreading of hilar cholangiocarcinoma by MDCT is reported.[37] In this study, we deliberately assessed the size of rMPD-type IPMNs, taking into account lateral spreading of papillary lesions, which is reflected on subtle brushlike appearance along the wall of pancreatic ducts (Figs. 2A, B). Measuring the radiological size of all IPMNs on CT images, we could conduct the analysis without separating rBD-type from rMPD/mixed-type IPMN. In addition, our diagnostic score (Table 5A) calculates an extensive MPD-type IPMN (>4 cm in size) as a score of 2 or more and indicates an immediate resection in a surgically fit patient, according to our treatment algorithm (Fig. 4). This is in line with the international consensus guideline,[6] in which all the MPD-type IPMNs are recommended to resection. Thus, actually, the discrimination between BD type and MPD/mixed type is integrated in our scoring system, together with the other 2 predictors (IPMN size and the presence of mural nodule or thick septum).

The number of patients with multifocal IPMNs is relatively small (5 patients) perhaps because the lesion was diagnosed as multiple only when multiple IPMNs were demonstrated pathologically in the resected specimen. For example, when a patient who had 2 suspected IPMN lesions in the pancreatic head and tail underwent pancreaticoduodenectomy and the resected specimen revealed a single IPMN in the pancreatic head, the patient was recognized as having a single IPMN lesion in our analysis because the diagnosis of the tail lesion has not been acquired pathologically.

This study was limited in that it was retrospective and evaluated the predictive ability of CT images for lesions known to be IPMNs. In addition, the study population is composed only of patients who underwent surgical resection. We intend to test our preoperative diagnostic algorithm using another large series of samples or in a prospective study.

ACKNOWLEDGMENT

The authors thank Dr Hidenori Ojima for useful discussions.

REFERENCES

1. Hruban RH, Pitman MB, Klimstra DS. *AFIP Atlas of Tumor Pathology Fourth Series Fascicle 6: Tumor of the Pancreas*. Washington, DC: American Registry of Pathology; 2007:75–110.
2. Longnecker DS, Adler G, Hruban RH, et al. Intraductal papillary-mucinous neoplasms of the pancreas. In: Hamilton SR, Aaltonen LA, eds. *Pathology and Genetics. Tumours of the Digestive System. World Health Organization Classification of Tumours*. Lyon, France: IARC Press; 2000:237–240.
3. Biankin AV, Kench JG, Dijkman FP, et al. Molecular pathogenesis of precursor lesions of pancreatic ductal adenocarcinoma. *Pathology*. 2003;35:14–24.
4. Hruban RH, Takaori K, Klimstra DS, et al. An illustrated consensus on the classification of pancreatic intraepithelial neoplasia and intraductal papillary mucinous neoplasms. *Am J Surg Pathol*. 2004;28:977–987.
5. Hiraoka N, Onozato K, Kosuge T, et al. Prevalence of FOXP3$^+$ regulatory T cells increases during the progression of pancreatic ductal adenocarcinoma and its precursor lesions. *Clin Cancer Res*. 2006;12:5423–5434.
6. Tanaka M, Chari S, Adsay V, et al. International consensus guidelines for management of intraductal papillary mucinous neoplasms and mucinous cystic neoplasms of the pancreas. *Pancreatology*. 2005;6:17–32.
7. Sakorafas GH, Sarr MG, van de Velde CJ, et al. Intraductal papillary mucinous neoplasms of the pancreas: a surgical perspective. *Surg Oncol*. 2005;14:155–178.
8. Murakami Y, Uemura K, Hayashidani Y, et al. Predictive factors of malignant or invasive intraductal papillary-mucinous neoplasms of the pancreas. *J Gastrointest Surg*. 2007;11:338–344.
9. Hara T, Yamaguchi T, Ishihara T, et al. Diagnosis and patient management of intraductal papillary-mucinous tumor of the pancreas by using peroral pancreatoscopy and intraductal ultrasonography. *Gastroenterology*. 2002;122:33–43.
10. Sugiyama M, Izumisato Y, Abe N, et al. Predictive factors for malignancy in intraductal papillary-mucinous tumours of the pancreas. *Br J Surg*. 2003;90:1244–1249.
11. Jang JY, Kim SW, Ahn YJ, et al. Multicenter analysis of clinicopathologic features of intraductal papillary mucinous tumor of the pancreas: is it possible to predict the malignancy before surgery? *Ann Surg Oncol*. 2005;12:124–132.
12. Sahani DV, Kadavigere R, Blake M, et al. Intraductal papillary mucinous neoplasm of pancreas: multi-detector row CT with 2D curved reformations—correlation with MRCP. *Radiology*. 2006;238:560–569.
13. Chari ST, Yadav D, Smyrk TC, et al. Study of recurrence after surgical resection of intraductal papillary mucinous neoplasm of the pancreas. *Gastroenterology*. 2002;123:1500–1507.
14. D'Angelica M, Brennan MF, Suriawinata AA, et al. Intraductal papillary mucinous neoplasms of the pancreas: an analysis of clinicopathologic features and outcome. *Ann Surg*. 2004;239:400–408.
15. Maire F, Hammel P, Terris B, et al. Prognosis of malignant intraductal papillary mucinous tumours of the pancreas after surgical resection. Comparison with pancreatic ductal adenocarcinoma. *Gut*. 2002;51:717–722.
16. Raimondo M, Tachibana I, Urrutia R, et al. Invasive cancer and survival of intraductal papillary mucinous tumors of the pancreas. *Am J Gastroenterol*. 2002;97:2553–2558.
17. Salvia R, Fernandez-del Castillo C, Bassi C, et al. Main-duct intraductal papillary mucinous neoplasms of the pancreas: clinical predictors of malignancy and long-term survival following resection. *Ann Surg*. 2004;239:678–687.
18. Shimada K, Sakamoto Y, Sano T, et al. Invasive carcinoma originating in an intraductal papillary mucinous neoplasm of the pancreas: a clinicopathologic comparison with a common type of invasive ductal carcinoma. *Pancreas*. 2006;32:281–287.
19. Sohn TA, Yeo CJ, Cameron JL, et al. Intraductal papillary mucinous neoplasms of the pancreas: an updated experience. *Ann Surg*. 2004;239:788–789.
20. Japan Pancreas Society. *Classification of Pancreatic Cancer*. 2nd ed. Tokyo: Kanehara; 2003.

21. Suzuki Y, Atomi Y, Sugiyama M, et al. Cystic neoplasm of the pancreas: a Japanese multiinstitutional study of intraductal papillary mucinous tumor and mucinous cystic tumor. *Pancreas*. 2004;28:241–246.

22. Nakagohri T, Kinoshita T, Konishi M, et al. Surgical outcome of intraductal papillary mucinous neoplasms of the pancreas. *Ann Surg Oncol*. 2007;14:3174–3180.

23. Nara S, Shimada K, Kosuge T, et al. Minimally invasive intraductal papillary-mucinous carcinoma of the pancreas: clinicopathological study of 104 intraductal papillary-mucinous neoplasms. *Am J Surg Pathol*. 2008;32:243–255.

24. Itai Y, Minami M. Intraductal papillary-mucinous tumor and mucinous cystic neoplasm: CT and MR findings. *Int J Gastrointest Cancer*. 2001;30:47–63.

25. Kawamoto S, Lawler LP, Horton KM, et al. MDCT of intraductal papillary mucinous neoplasm of the pancreas: evaluation of features predictive of invasive carcinoma. *Am J Roentgenol*. 2006;186:687–695.

26. Nakagohri T, Konishi M, Inoue K, et al. Invasive carcinoma derived from intraductal papillary mucinous carcinoma of the pancreas. *Hepatogastroenterology*. 2004;51:1480–1483.

27. Matsumoto T, Aramaki M, Yada K, et al. Optimal management of the branch duct type intraductal papillary mucinous neoplasms of the pancreas. *J Clin Gastroenterol*. 2003;36:261–265.

28. Kobayashi G, Fujita N, Noda Y, et al. Mode of progression of intraductal papillary-mucinous tumor of the pancreas: analysis of patients with follow-up by EUS. *J Gastroenterol*. 2005;40:744–751.

29. Salvia R, Crippa S, Falconi M, et al. Branch-duct intraductal papillary mucinous neoplasms of the pancreas: to operate or not to operate? *Gut*. 2006;56:1086–1090.

30. Kimura W. IHPBA in Tokyo, 2002: surgical treatment of IPMT vs MCT: a Japanese experience. *J Hepatobiliary Pancreat Surg*. 2003;10: 156–162.

31. Sugiyama M, Atomi Y, Hachiya J. Intraductal papillary tumors of the pancreas: evaluation with magnetic resonance cholangiopancreatography. *Am J Gastroenterol*. 1998;93:156–159.

32. Irie H, Honda H, Aibe H, et al. MR cholangiopancreatographic differentiation of benign and malignant intraductal mucin-producing tumors of the pancreas. *Am J Roentgenol*. 2000;174:1403–1408.

33. Scaglione M, Pinto A, Romano S, et al. Using multidetector row computed tomography to diagnose and stage pancreatic carcinoma: the problems and the possibilities. *J Pancreas*. 2005;6:1–5.

34. Prokesch RW, Schima W, Chow LC, et al. Multidetector CT of pancreatic adenocarcinoma: diagnostic advances and therapeutic relevance. *Eur Radiol*. 2003;13:2147–2154.

35. Balthazar EJ. Pancreatitis associated with pancreatic carcinoma. *Pancreatology*. 2005;5:330–344.

36. Couvelard A, Sauvanet A, Kianmanesh R, et al. Frozen sectioning of the pancreatic cut surface during resection of intraductal papillary mucinous neoplasms of the pancreas is useful and reliable. *Ann Surg*. 2005; 242:774–778.

37. Unno M, Okumoto T, Katayose Y, et al. Preoperative assessment of hilar cholangiocarcinoma by multidetector row computed tomography. *J Hepatobiliary Pancreat Surg*. 2007;14:434–440.

Surg Today (2009) 39:32–37
DOI 10.1007/s00595-008-3814-7

SURGERY TODAY

Roux-en-Y Reconstruction Using Staplers During Pancreaticoduodenectomy: Results of a Prospective Preliminary Study

YOSHIHIRO SAKAMOTO, TAKAHIRO KAJIWARA, MINORU ESAKI, KAZUAKI SHIMADA, SATOSHI NARA, and TOMOO KOSUGE

Hepatobiliary and Pancreatic Surgery Division, National Cancer Center Hospital, 5-1-1 Tsukiji, Chuo-ku, Tokyo 104-0045, Japan

Abstract

Purpose. The aim of this study was to reveal the utility of alimentary reconstruction using staplers during pancreaticoduodenectomy (PD), focusing on the occurrence of delayed gastric emptying.

Methods. Between 2003 and 2007, 72 PDs with alimentary reconstruction were performed by a single surgeon. Since August 2006, the new Roux-en-Y reconstruction methods using staplers were applied in 26 of the patients. We compared their clinical outcomes with those of the 46 patients who underwent PD using the conventional hand-sewn reconstruction methods.

Results. The results of upper gastrointestinal study showed improvement within 10 postoperative days (PODs; $P = 0.03$): the patients resumed eating their regular diet sooner (13 vs 6 days, $P < 0.001$), and both the incidence of delayed gastric emptying (43% vs 19%, $P = 0.04$) and the hospital stay (27 vs 21 days, $P = 0.008$) were reduced significantly in patients with stapled reconstruction. Despite the fact that operative costs were significantly higher for patients with stapled reconstruction ($P = 0.009$), hospital costs were significantly lower ($P = 0.049$) for those who underwent the conventional method.

Conclusions. Our retrospective analysis shows that stapled reconstructions might reduce the incidence of delayed gastric emptying; however, further study will be necessary to evaluate the utility of this new method.

Key words Pancreaticoduodenectomy · Delayed gastric emptying · Stapled reconstruction · Roux-en-Y reconstruction · Hospital stay

Reprint requests to: Y. Sakamoto
Received: April 2, 2008 / Accepted: May 28, 2008

Introduction

Alimentary reconstruction using staplers during gastric and colorectal surgery is widely accepted. The use of circular staplers in esophagojejunostomy is more convenient and safer than hand-sewn suturing.[1] Moreover, colorectal anastomoses using a double stapling technique have also become popular,[2] especially since the advent of laparoscopic surgery.[3] However, to our knowledge, mechanical reconstruction using staplers during pancreatectomy has never been documented.

One of the most common complications of pancreaticoduodenectomy (PD) is delayed gastric emptying (DGE), otherwise known as "gastroparesis,"[4] which is not fatal but results in prolonged hospital stay and increased hospital costs. Delayed gastric emptying is defined as nasogastric decompression after postoperative day (POD) 10 or a failure to tolerate a regular diet after POD 14. The incidence of DGE has been reported to range from 5% to 72%.[5–13] We hypothesized that the hand-sewn, two-layered, or continuous suture could induce anastomotic edema, which is one of the causes of DGE. Mechanical alimentary reconstruction can prevent anastomotic edema and may keep the oral intake stable. Therefore, in August 2006, we introduced a new Roux-en-Y reconstruction method, which uses circular or linear staplers during PD. We report the preliminary results of our new method.

Patients and Methods

Between August 1, 2003 and September 30, 2007, 302 patients underwent PD in our institute. These operations were performed by one or more of five surgeons, so to maintain consistency we evaluated the surgical outcomes of the 76 PDs performed by a single surgeon (Y.S.). Between August 2003 and July 2006, 50 patients underwent PD with alimentary reconstruction using the

conventional hand-sewn method. The new stapled Roux-en-Y reconstruction method was introduced in August 2006, and 26 patients underwent mechanical reconstruction in the final year of the study. Among the 50 patients operated on during the former 3 years, the following four patients were excluded from the analysis: two who had undergone previous gastrojejunostomy, one who had undergone previous total gastrectomy, and one who underwent PD concomitant with total gastrectomy.

The underlying diseases were as follows: invasive pancreatic cancer in 41 patients, bile duct cancer in 12 patients, ampullary cancer in 7 patients, intraductal papillary mucinous tumor in 3 patients, neuroendocrine tumor in 2 patients, metastatic cancers in 2 patients, duodenal cancer in 1 patient, and other noncancerous diseases in 4 patients. The surgical procedures consisted of standard Whipple procedure (SW) in 22 patients and pylorus-preserving pancreaticoduodenectomy (PPPD) in 50 patients. Twenty patients (28%) underwent combined portal vein resection. One patient underwent concomitant extended right hemihepatectomy, and another underwent concomitant distal pancreatectomy.

The surgical outcomes of PD, including the occurrence of DGE and other surgical complications, were compared between the 46 patients who underwent PD using conventional reconstruction and the 26 patients who underwent the new Roux-en-Y stapled reconstruction. The backgrounds and surgical procedures of each group are summarized in Table 1.

Surgical Technique of PD

The details of the standard procedure for PD have been described elsewhere.[14] After removal of the pancreatic head, we wrapped the stump of the gastroduodenal artery using the falciform ligament to prevent the bleeding caused by pancreatic leakage.[15] A jejunal loop was lifted and pancreaticojejunostomy was performed by duct-to-duct anastomosis using 5-0 polydioxanone (PDS). The anterior and posterior pancreatic walls were tightly affixed to the jejunal serosa using interrupted 4-0 PDS sutures. A hepaticojejunostomy was then done using interrupted 5-0 PDS sutures.

Conventional Reconstruction

In the 46 conventional PDs, we performed an antecolic gastrojejunostomy and duodenojejunostomy during the standard Whipple procedure (SW, $n = 16$) and pylorus-preserving pancreaticoduodenectomy (PPPD, $n = 30$), respectively. These anastomoses were done on antecolic routes, by the Albert–Lembert ($n = 38$), layer to layer ($n = 6$), or Gambee ($n = 2$) methods. A Braun jejunojejunostomy was done to prevent direct exposure of the anastomotic site to pancreatic and bile juice. Gastric tubes ($n = 43$) and jejunal feeding tubes ($n = 45$) were pulled out through the afferent loop between the duodeno- or gastrojejunostomy and Braun anastomosis. External drainage of the pancreatic and biliary ducts was performed in all of the patients.

Roux-en-Y Reconstruction Using a Circular Stapler During Pylorus-Preserving Pancreaticoduodenectomy (PPPD)

An antecolic duodenojejunostomy was performed by Roux-en-Y reconstruction using a circular stapler in 20 PPPDs (Proximate ILS 29 or 25 mm, Ethicon Endo-Surgery, Cincinnati, OH [$n = 19$], EEA circular stapler,

Table 1. Clinical characteristics of patients who underwent conventional versus Roux-en-Y stapled reconstruction

	Conventional ($n = 46$)	Roux-en-Y, stapled ($n = 26$)	P value
Sex			
Male	29	15	0.66
Female	17	11	
Age (years)	68 (18–82)	66 (47–80)	0.80
Body mass index	21 (15–28)	22 (17–27)	0.25
Diseases			
Pancreatic cancer	26	15	0.81
Bile duct cancer	7	5	
Vater or duodenal cancer	7	2	
Others	6	4	
Procedure			
SW	16	6	0.30
PPPD	30	20	
Portal vein resection			
Performed	14 (30%)	6 (23%)	0.50
Operative time (min)	560 (400–842)	570 (374–790)	0.77
Blood loss (ml)	850 (215–2360)	710 (130–2420)	0.19

SW, standard Whipple procedure; PPPD, pylorus-preserving pancreaticoduodenectomy